A new Griesbachian-Dienerian (Induan, Early Triassic) ammonoid fauna from Gujiao, South China.

Xu Dai, Haijun Song, Arnaud Brayard, David Ware

A new Griesbachian–Dienerian (Induan, Early Triassic) ammonoid fauna from Gujiao, South China

Xu Dai[1], Haijun Song[1]*, Arnaud Brayard[2], David Ware[3]

[1]State Key Laboratory of Biogeology and Environmental Geology, School of Earth Sciences, China University of Geosciences, Wuhan 430074, China. haijunsong@cug.edu.cn; xudai@cug.edu.cn

[2]Biogéosciences, UMR 6282, CNRS, Université Bourgogne Franche-Comté, 6 Boulevard Gabriel, 21000 Dijon, France. arnaud.brayard@u-bourgogne.fr

[3]Museum für Naturkunde, Leibniz Institute for Evolution and Biodiversity Science, Invalidenstrasse 43, 10115 Berlin, Germany. david.ware@mfn-berlin.de

*Corresponding author. Email: haijunsong@cug.edu.cn

Running Header: A new Induan ammonoid fauna from South China

Abstract.—Bed-by-bed sampling of the lower portion of the Daye Formation at Gujiao, Guizhou Province, South China, yielded new Griesbachian–Dienerian (Induan, Early Triassic) ammonoid faunas showing a new regional Induan ammonoid succession. This biostratigraphic scheme includes in chronological order the late Griesbachian *Ophiceras medium* and *Jieshaniceras guizhouense* beds, and the middle Dienerian *Ambites radiatus* bed.

The latter is recognized for the first time as a separate biozone in South China. Eight genera and 13 species are identified, including one new species, *Mullericeras gujiaoense* n. sp. The new data show that a relatively high level of ammonoid taxonomic richness occurred rather rapidly after the Permian/Triassic mass extinction in the late Griesbachian, echoing similar observations in other basins, such as in the Northern Indian Margin.

Introduction

The Permian/Triassic (PT) boundary witnessed the largest biotic crisis among all Phanerozoic mass extinctions, resulting in the 80% to 90% extirpation of marine species (Raup, 1979; Song et al., 2013; Stanley, 2016). This major event coincided with high temperatures (Joachimski et al., 2012; Sun et al., 2012; Romano et al., 2013), potential anoxia (Wignall and Twitchett, 1996; Song et al., 2012) and acidification (Clarkson et al., 2015) in the oceans, as well as pronounced perturbations in the carbon cycle (Payne et al., 2004; Galfetti et al., 2007) and intensified continental weathering (Algeo and Twitchett, 2010; Song et al., 2015a). Following the PT mass extinction, a delayed recovery has often been proposed (Hallam, 1991; Tong et al., 2007; Chen and Benton, 2012). However, studies of some groups, such as conodonts, ammonoids and foraminifers, show that the recovery was well underway by at least the Smithian (Orchard, 2007; Brayard et al., 2009; Song et al., 2011), i.e., less than 1 million years after the PT mass extinction (Galfetti et al. 2007; Baresel et al. 2017). Some assemblages documenting relatively high taxonomic richness during the late Griesbachian–early Dienerian also challenge previous claims of a globally delayed recovery

45 (Twitchett et al., 2004; Foster et al., 2017; Ware et al., 2015; Wang et al., 2017).

46 To decipher the causes of the PT crisis and associated recovery patterns and processes, a
47 high-resolution biostratigraphic frame is a prerequisite. With coupled high origination and
48 extinction rates, the ammonoid turnover was extremely fast in the Early Triassic (Brayard et
49 al., 2006, 2009; Brühwiler et al., 2010; Ware et al., 2015). Ammonoids are, therefore, one of
50 the most useful index fossil for biostratigraphy in this interval (Jenks et al., 2015). For
51 example, on the Northern Indian Margin, a total of 12 and 14 regional ammonoid Unitary
52 Associations have been recognized for the Dienerian and Smithian, respectively (Brühwiler et
53 al., 2010, 2011; Ware et al., 2015); this represents an unprecedented high-resolved
54 biostratigraphic scale, compared with coeval records from other regions, such as the western
55 USA basin, with six Smithian ammonoid Unitary Associations (Jattiot et al., 2017; Jenks &
56 Brayard 2018).

57 South China is renowned for its PT marine and terrestrial records and the Global
58 Stratotype Section and Point (GSSP) of the PT boundary is located at Meishan, Zhejiang
59 Province (Yin et al., 2001). In the past 50 years, approximately 100 geological sections
60 spanning the PT boundary and the Early Triassic have been documented in South China, and
61 represent various shallow to deep-marine environments (e.g., Brayard and Bucher, 2008;
62 Galfetti et al., 2008; Song et al., 2011; Bai et al., 2017; Wang et al., 2017). Based on these
63 rather exhaustive environmental records, many clades and geochemical proxies were studied
64 to decipher the regional biotic recovery signal. The diversity of both benthic and nektonic
65 organisms was analyzed mainly based on foraminifers (Song et al., 2011, 2015b),
66 brachiopods (Chen et al., 2015; Wang et al., 2017), bivalves (Yin, 1985; Huang et al., 2014),

gastropods (Pan et al., 2003; Kaim et al., 2010), conodonts (Zhao et al., 2007; Zhang et al., 2007; Jiang et al., 2014; Brosse et al., 2015, 2016; Liang et al., 2016; Bai et al., 2017) and ammonoids (Chao, 1959; Xu, 1988; Mu et al., 2007; Brühwiler et al., 2008; Brayard and Bucher, 2008). Paleoenvironmental and paleoclimatic signals were also intensively studied from numerous South Chinese sections (Payne et al., 2004; Galfetti et al., 2007, 2008; Song et al., 2012, 2017). Regarding these studies, the biostratigraphic framework used is crucial for correlation among different biotic and environmental signals and between distant areas. Nevertheless, there are only a limited number of ammonoid biostratigraphic schemes that have been proposed for the Early Triassic of South China (e.g., Tong and Wu, 2004; Galfetti et al., 2007; Brayard and Bucher, 2008; Brühwiler et al., 2008).

Early Triassic ammonoid faunas in South China have been sporadically studied over the last 80 years. Tien (1933) initially described some ammonoid specimens from Hubei and Guizhou provinces. Then, Hsü (1937) reported a few ammonoid taxa based on deformed specimens from Jiangsu, Zhejiang and Hubei provinces. In 1959, Chao illustrated a diverse, well-preserved ammonoid fauna from Guangxi, but with only rare Griesbachian and Dienerian specimens. Since the work of Chao (1959), a few Early Triassic ammonoid faunas were described (Mu et al., 2007; Tong and Wu, 2004; Xu, 1988). Due to their relatively poor preservation and spatio-temporally restricted occurrences, the taxonomy, biostratigraphy and diversity patterns of ammonoids from South China remained largely imperfectly known until recently. New ammonoid material from Guangxi and Guizhou provinces provided a biostratigraphic framework for small parts of the Griesbachian and Dienerian and for the Smithian–Spathian interval (Galfetti et al., 2007; Brühwiler et al., 2008; Brayard and Bucher,

2008). However, the preliminary Griesbachian–Dienerian (Induan) zonation remained poorly resolved with many uncertainties for large-scale correlation among distant basins. In sum, our knowledge of the Griesbachian–Dienerian ammonoid taxonomy and biostratigraphy based on South Chinese data is fragmented.

Here, we document a new Griesbachian-Dienerian ammonoid succession based on bed-by-bed sampling of the Gujiao section, which can complement previous regional biostratigraphic schemes and can help correlation with other worldwide zonations.

Geological setting

The Gujiao section is located ~ 20 km southeast from Guiyang, the capital of the Guizhou Province, South China. During the Early Triassic, it was located in the transitional zone between the Yangtze Platform and the Nanpanjiang Basin (Fig. 1). A new and well-exposed outcrop was excavated in 2015 along a new road, which exposed Permian and Triassic strata (Fig. 2). These exposures include the Upper Permian Changxing and Dalong formations and the Lower Triassic Daye Formation.

The Changxing Formation consists of massive bioclastic and cherty limestones (Zhao et al., 1978), yielding abundant and diverse typical Permian organisms, such as brachiopods, gastropods, corals, dasycladacean algae, ammonoids (Zhao et al., 1978; Zheng, 1981), and foraminifers, indicating a well-developed carbonate platform environment.

At Gujiao, the Dalong Formation is ~ 10 m in thickness and is dominated by cherty limestones, siliceous mudstones alternating with black or gray shales and volcanic ash beds,

representing a deeper basinal environment. At the bottom of the Dalong Formation, a ~30 cm-thick limestone bed contains abundant and well-preserved ammonoids with e.g., *Pseudotirolites* and *Pseudogastrioceras*, indicating a late Changhsingian age (Zhao et al., 1978).

The lower part of the Triassic Daye Formation is ~50 m-thick and consists of marlstones interbedded with shales. It directly overlies the Dalong Formation without an apparent unconformity, although earliest Griesbachian ammonoids are missing. Abundant ammonoid and bivalve specimens as well as some gastropods were collected in the lowermost 6 m. Trace fossils also occasionally occur. Ammonoids from shales are deformed and cannot be identified. Although generally difficult to extract from the argillaceous limestones, recrystallized ammonoid specimens were abundantly sampled from bed GJ-40. Based on observed facies, the lower Daye Formation corresponds to a basin or basin-margin environment.

Materials

A total of 749 ammonoid specimens were collected. Although often not well preserved, they represent 8 genera and 13 species (Fig. 3), including *Ophiceras medium* Griesbach, 1880, *Ophiceras* sp. indet., *Vishnuites pralambha* Diener, 1897, Ophiceratidae gen. indet., *Ambites radiatus* (Brühwiler et al., 2008), Gyronitidae gen. et sp. indet., ?Gyronitidae gen. et sp. indet., *Proptychites* sp. indet., *Pseudoproptychites* cf. *hiemalis* (Diener, 1895), *Jieshaniceras guizhouense* (Zakharov and Mu in Mu et al., 2007), *Mullericeras gujiaoense* n. sp.,

Ussuridiscus cf. *varaha*, and ?Mullericeratidae gen. indet.

Repository and institutional abbreviation.— YFMCUG: Yifu Museum of China University of Geosciences, Wuhan.

Systematic paleontology

Systematic descriptions mainly follow the classification established by Tozer (1994) and refined by Brühwiler et al. (2008) and Ware et al. (2011and in press). Synonymy lists and taxa in open nomenclature are annotated following the recommendations of Matthews (1973) and Bengtson (1988). 'v' implies that the authors have checked the original material of the reference; 'p' indicates that the reference applies only in part to the species under discussion. The morphological range of each taxon is quantified using the four classic geometrical parameters of the ammonoid shell: diameter (D), whorl height (H), whorl width (W) and umbilical diameter (U).

Order Ceratitida Hyatt, 1884

Family Ophiceratidae Arthaber, 1911

Genus *Ophiceras* Griesbach, 1880

Type species.—*Ophiceras tibeticum* Griesbach, 1880 from Shalshal Cliff, Painkhanda, Niti region, Himalayas, India.

155

156 *Remarks*.—*Ophiceras* is the most abundant and widely distributed genus among the
157 Ophiceratidae. It differs from *Vishnuites*, *Wordieoceras* and *Shangganites* by a distinct
158 rounded venter and from *Discophiceras*, *Ghazalaites* and *Kyoktites* by a more evolute conch.
159 It has a broad paleogeographic distribution with numerous species described from both the
160 Tethys area (South China, Spiti, Kashmir, Salt Range and South Tibet) and high-latitude
161 regions, such as Greenland and Arctic Canada. *Ophiceras* was first documented by Griesbach
162 (1880) from the *Otoceras* beds at Shalshal Cliff in Himalaya. Diener (1897) then described
163 10 species of *Ophiceras* from the Himalayas (mostly from Shalshal Cliff) and divided them
164 into two groups, the *O. tibeticum* and the *O. sakuntala* groups, essentially based on their
165 different shell ornamentation. The *O. tibeticum* group displays some relatively low folds,
166 sometimes becoming nodes near the umbilical shoulder, whereas the *O. sakuntala* group
167 usually exhibits a smooth shell, with only fine growth lines. In addition, species of the *O.*
168 *tibeticum* group are usually more evolute than those of the *O. sakuntala* group. As noticed by
169 Diener (1897), there is no distinct boundary between the two groups, and some species might
170 be variants of other ones. Kummel (1972) took intraspecific variability into account and
171 proposed only three valid species: *O. tibeticum*, *O. serpentinum* and *O. medium*. His
172 discussion was short, but he provided illustrations of Diener's (1897) type material and of
173 additional unpublished material. However, Kummel's (1972) revision is based on specimens
174 in old collections lacking detailed stratigraphic context (i.e., without bed-by-bed collecting),
175 and given the stratigraphic uncertainty must be considered with caution. Here, in the absence
176 of a proper revision of these faunas, the opinion of Kummel (1972) is followed.

177 Spath (1930, 1935) described several new species of *Ophiceras* from East Greenland.
178 He proposed several subgenera such as *Lytophiceras*, *Discophiceras*, *Metophiceras* and
179 *Acanthophiceras*. Trümpy (1969) included *Metophiceras* in Xenodiscidae, erected
180 *Discophiceras* as a full genus, and considered *Lytophiceras* and *Acantophiceras* as synonyms
181 of *Ophiceras*, rejecting the sub-generic subdivision of *Ophiceras*. Tozer (1994) illustrated
182 several forms of *Ophiceras* from Arctic Canada, which are identical to those from East
183 Greenland. *Ophiceras* specimens from South China are usually poorly preserved or juvenile
184 specimens too small for a proper identification, thus making comparison with other regions
185 difficult. The relationships of *Ophiceras* faunas among Himalayas, Arctic Canada, East
186 Greenland and South China remain unclear.
187
188 *Ophiceras medium* Griesbach, 1880
189 Figure 4.1–4.11
190
191 1880 *Ophiceras medium* Griesbach, p. 111, pl. 3, fig. 9.
192 1880 *Trachyceras* (?) *gibbosum* Griesbach, p. 111, pl. 3, fig. 10
193 1897 *Ophiceras gibbosum*; Diener, 108–110, pl. 9, fig. 47.
194 1897 *Ophiceras platyspira* Diener, p. 113, pl. 12, figs 5, 6.
195 1897 *Ophiceras sakuntala* Diener, p. 114–118, pl. 10, figs 1–7; pl. 11, figs 1, 2, 4.
196 1897 *Ophiceras medium*; Diener, p. 118, pl. 9, figs 1–2.
197 1897 *Ophiceras ptychodes* Diener, p. 120–121, pl. 11, figs 3, 5, 6.
198 1897 *Ophiceras demissum*; Diener, p. 121–123, pl. 14, figs 1–7.

1897 *Ophiceras chamunda* Diener, p. 123–125, pl. 12, figs 1–4.

? 1913 *Ophiceras sakuntala*; Diener, p. 15–16, pl. 1, figs 1–2.

? 1933 *Ophiceras tingi* Tien, p. 9, pl. 1, figs 4a–c.

? 1937 *Ophiceras* sp.; Hsü, p. 319, pl. 2, figs 4–5.

1972 *Ophiceras medium*; Kummel, pl. 7, figs 1–13; pl. 8, figs 1–16; pl. 9, figs 1–14; pl. 10, figs 1–18.

1976 *Ophiceras* (*Lytophiceras*) *sakuntala*; Wang and He, p. 272, pl. 2, figs 4–6; p. 270, text-fig. e.

2003 *Ophiceras* cf. *sakuntula*; Krystyn et al., p. 336, fig. 4D.

? 2004 *Ophiceras* sp.; Tong and Wu, p. 196, pl. 1, figs 3–5.

? 2004 *Lytophiceras* sp.; Tong and Wu, p. 196, pl. 1, fig. 6.

? 2006 *Lytophiceras* cf. *chamunda*; Bu et al., fig. 3c.

? 2006 *Ophiceras tingi*; Bu et al., figs 3h–i.

? 2006 *Ophiceras* sp.; Bu et al., figs 3g, j, k.

? 2009 *Ophiceras* sp.; Zhang et al., fig. 5j.

? 2009 *Hypophiceras* sp.; Zhang et al., fig. 5k.

? 2009 *Lytophiceras* sp.; Zhang et al., fig. 5l.

Lectotype.—GSI 5973 (Griesbach, 1880, pl. 3, fig. 9; Diener, 1897, pl. 9, fig. 2; Kummel, 1972, pl. 8, figs 15–16), from the *Otoceras* beds at Rimkin Paiar encamping ground, Shalshal Cliff, Painkhanda, Niti region, Himalayas, India.

Occurrence.—Late Griesbachian. Himalayas (Griesbach, 1880; Diener, 1897 and Wang and He, 1976), South China (this work).

Description.—Discoidal, relatively involute and compressed (W/H≈0.58, W/D≈0.26) shell displaying a growth allometry with coiling becoming more evolute during ontogeny. The largest specimen sampled at Gujiao displays a U/D≈0.36, while the smaller displays a ratio of ~ 0.25 (Fig. 5). The venter is narrow and rounded, without distinct ventro-lateral shoulders. Flanks slightly convex with maximum whorl width near the inner third of the flanks. The umbilical wall is moderately deep with a rounded shoulder. The flanks only exhibit fine slightly curved growth lines. Suture line ceratitic. The ventral lobe is shallow with two pointed branches. The first lateral lobe is twice as deep as the second lateral lobe. Both of them show fine indentations at their base. Saddles are rounded and the second lateral saddle is slightly asymmetric.

Material.—Three specimens from bed GJ-15, one specimen from bed GJ-28 and several questionable specimens from beds GJ-13, GJ-14, GJ-20, GJ-22, GJ-23 and GJ-27 (Fig. 3). Registered specimens: YFMCUG 00001, YFMCUG 00002, YFMCUG 00003 and YFMCUG 00008.

Remarks.—Our specimens differ from *O. tibeticum* in that the shell is more involute with smooth flanks, and from *O. serpentinum* by a more compressed and involute shell. Previous descriptions of *Ophiceras* from South China are based on very poorly preserved specimens,

so their assignment is often questionable, preventing their use for further discussion. Described specimens are typically severely deformed, without suture lines and visible venter (e.g., Zhang et al., 2009, fig. 5j) and may be confused with smooth gyronitids for instance. Thus, these deformed specimens were not included in our taxonomic discussion. In South China, *O. tingi* was first described by Tien (1933) and is morphologically close to *O. medium*. *O. tingi* is characterized by an unusual 'V' shaped second lateral lobe, which is most probably the result of intense weathering or degradation during preparation of the suture line. *O. sinense* documented from Guiyang (Tien, 1933) shows some fine folds and nodules near the umbilical shoulder, which correspond to some forms of *O. tibeticum* from Himalayas. No well-preserved specimens of this species were retrieved and its validity is questioned. Brühwiler et al. (2008) reported several well-preserved juvenile specimens of *Ophiceras* with some ribs from Guangxi Province, which might be juvenile individuals of *O. sinense*. However, due to their small size and in the absence of study concerning their ontogeny, this remains an open question. An in-depth review of *Ophiceras* from South China with better-preserved specimens would be necessary to decipher its taxonomy.

Ophiceras sp. indet.

Figure 4.12–4.18

? 1988 *Gyrophiceras plicatum*; Xu, p. 446, pl. 2, fig. 7.

? 2007 *Gyrophiceras subplicatum*; Zakharov and Mu in Mu et al., p. 866, figs 10.10–16, 19, 11.2–3.

Occurrence.—Late Griesbachian of South China.

Description.—Sub-evolute (U/D≈0.38), serpenticonic (W/D≈0.3) shell with a sub-circular (W/H≈0.8) whorl section (Fig. 6), and an arched venter with rounded ventro-lateral shoulders. Flanks convex with maximum whorl width near mid-flanks. Umbilicus is broad and moderately deep with a low vertical umbilical wall and a rounded umbilical shoulder. No ornamentation visible on our specimens, but this might be due to their poor preservation. Suture line not sufficiently preserved to be drawn and described.

Material.—Very abundant in bed GJ-33. Registered specimens: YFMCUG 00052-00084.

Remarks.—Similar specimens have been reported from South China and assigned to *Gyrophiceras plicatum* and *G. subplicatum* (Xu, 1988; Mu et al., 2007). *Gyrophiceras* was erected by Spath (1934) based on the species *Lecanites gangeticus* Waagen, 1895 (holotype on pl. 39, figs. 4a–c.), and assigned to Gyronitidae. However, according to the taxonomic revision of Gyronitidae by Ware *et al*. (in press), the holotype is a pathological specimen which most probably belongs to *Gyronites*, so, *Gyrophiceras* is considered invalid. Specimens from South China assigned to *Gyrophiceras* by Xu (1988) and by Zakharov & Mu (2007) belong to different genera and families. Xu (1988) reported three species of *Gyrophiceras*: *G. hubeiense*, *G. orientale* and *G. plicatum*, but only the latter is similar to our specimens. *G. hubeiense* and *G. orientale* are more involute and thicker than our specimens.

G. subplicatum (Zakharov and Mu in Mu et al., 2007) does not exhibit any marked difference with our specimens, and thus may be considered synonymous. *G. plicatum* was initially described by Chao (1959) from Smithian specimens, which likely belong to *Dieneroceras*. The Induan specimens assigned by Xu (1988) and Zakharov and Mu (in Mu et al., 2007) to *G. plicatum* were thus likely misidentified and actually correspond to an undetermined *Ophiceras* species. As our specimens and Xu's material are too poorly preserved and small to establish if they are a new species, or if they are juveniles of another *Ophiceras* species, whose ontogeny is unknown (e.g., *O. serpentinum*), we prefer to keep this taxon in open nomenclature.

Genus *Vishnuites* Diener, 1897

Type species.—*Vishnuites pralambha* Diener, 1897

Remarks.—This ophiceratid genus is characterized by an acute venter. A detailed discussion of this genus is available in Brühwiler et al. (2008).

Vishnuites pralambha Diener, 1897

Figure 4.21–4.23

1897 *Xenaspis* (*Vishnuites*) *pralambha* Diener, p. 88, pl. 7, figs 4–5.

? 1959 *Vishnuites marginalis* Chao, p. 190, pl. 11. figs 17–18.

1972 *Vishnuites pralambha*; Kummel, pl. 12, figs 1–4.

? 1988 *Vishnuites huazhongensis* Xu, p. 441, pl. 1, fig. 8, text-fig. 6.

? 1988 *Vishnuites lichuanensis* Xu, p. 441, pl. 1, fig. 3, pl. 2, fig. 10, text-fig. 7.

? 1988 *Vishnuites marginalis* Xu, p. 443, pl. 2, fig. 1, text-fig. 8.

? 1988 *Vishnuites orientalis* Xu, p. 443, pl. 2, fig. 6, text-fig. 9.

1988 *Vishnuites yangziensis* Xu, p. 444, pl. 1, fig. 9, pl. 2, fig. 3, text-fig. 10.

2007 *Vishnuites wenjiangsiensis* Zakharov and Mu in Mu et al., p. 860, figs 3.12–17, 5.1.

2007 *Vishnuites* cf. *yangziensis*; Zakharov and Mu in Mu et al., p. 860, figs 5.2, 6.3, 6.4, 6.6, 6.8, 6.10, 6.12.

v 2008 *Vishnuites pralambha*; Brühwiler et al., p. 1161, pl. 1, figs 18–21.

Lectotype.—GSI5950 (Diener, 1897, pl. 7, fig. 4; Kummel, 1972, pl. 12, fig. 1) from the *Otoceras* beds at Rimkin Paiar encamping ground, Shalshal Cliff, Painkhanda, Niti region, Himalayas, India.

Occurrence.—*Otoceras* beds of the Himalayas (Diener, 1897); late Griesbachian of South China (Xu, 1988; Mu et al., 2007; Brühwiler et al., 2008; this work).

Description.—Moderately evolute (U/D≈0.41) compressed shell, with an acute venter. Convex flanks with maximum whorl width at the middle of flanks. Umbilicus broad and shallow, with a low wall and a rounded umbilical margin. Ornamentation not preserved. Suture line very poorly preserved but remains of a developed auxiliary series is visible (see

Fig. 4.21).

Material.—Several specimens from beds GJ-24, GJ-25 and GJ-33, with only a single measurable specimen. Registered specimens: YFMCUG 00007 and YFMCUG 00051.

Remarks.—*Vishnuites* species erected by Chao (1959), Xu (1988) and Zakharov and Mu (in Mu et al., 2007) based on rather poorly preserved specimens from South China have been considered as synonyms of *V. pralambha* Diener, 1897 by Brühwiler et al. (2008). However, this genus and its species are poorly known. It has been erected from two fragmentary specimens, which lack detailed stratigraphic context. They were collected from Diener's (1978) "*Otoceras* beds" , which correspond to an interval encompassing the Griesbachian up to at least the middle Dienerian, and the Shalshal Cliff locality found at the border between India and China in the central Himalayas has not be re-investigated. The ontogeny, intraspecific variability, and exact stratigraphic position of this species thus remains unknown. We here decided to keep the name *Vishnuites pralambha* for specimens from South China despite minor differences from the holotype (e.g., slightly thicker whorl section, higher umbilical wall, longer auxiliary series) for continuity with previous works on South Chinese ammonoids. However, it is awaiting a proper revision to confirm or reject the synonymy between the material from South China and from central Himalaya. *Pseudovishnuites* Zakharov and Mu (in Mu *et al*. 2007) exhibits a wider and deeper ventral lobe with distinct adventitious elements, but was considered as a synonym of *Vishnuites* by Brühwiler et al. (2008). More material with well-preserved suture lines is needed to confirm the validity of

Pseudovishnuites. *V*. (‘*Paravishnuites*’) *oxynotus* and *V*. (‘*P*’) *striatus* described by Spath (1935) from East Greenland are relatively more involute and display fine radial folds on their flanks.

Ophiceratidae gen. indet.

Figure 4.19–4.20

Occurrence.—Lower Daye Formation, Guizhou, South China. *Ophiceras medium* beds, late Griesbachian.

Description.—Moderately involute, compressed shell with rounded venter, flanks slightly convex and maximum whorl width near the umbilical margin. Umbilicus small with an oblique wall and a rounded umbilical shoulder. Ornamentation not preserved. Suture line ceratitic. The ventral lobe is not visible. The first lateral lobe is rather deep, with small, regular denticulations at its base. First and second lateral saddles are elongated and slightly asymmetric. The third lateral saddle is short with a broad rounded tip. Auxiliary series is quite short with fine indentations.

Material.—A single specimen from bed GJ-23. Registered specimen: YFMCUG 00006.

Remarks.—This specimen is close to involute forms of Ophiceratidae, such as *Discophiceras*, *Ghazalaites* and *Kyoktites*. However, the poor preservation prevents further identification.

375

376 Family Gyronitidae Waagen, 1895

377 Genus *Ambites* Waagen, 1895

378

379 *Type species*.—*Ambites discus* Waagen, 1895 from Salt Range, Pakistan.

380

381 *Remarks*.—*Ambites* can be distinguished from *Gyronites* by its typical bottlenecked venter. A

382 detailed discussion of this genus can be found in Ware et al. (in press).

383

384 *Ambites radiatus* (Brühwiler et al., 2008)

385 Figures 7.1–7.16, 15.6

386

387 v 2008 *Pleurambites radiatus* Brühwiler et al., p. 1168, pl. 5, figs 1 (holotype), 2–3.

388 v [in press] *Ambites radiatus*; Ware et al., pl. 9, figs 11–28.

389

390 *Holotype*.—PIMUZ 26766 (Brühwiler et al., 2008, pl. 5, fig. 1) from Jinya, Guangxi, South

391 China.

392

393 *Occurrence*.—Middle Dienerian of the Northern Indian Margin (Ware et al., 2015) and South

394 China (Brühwiler et al., 2008; this work).

395

396 *Description*.—Small, sub-evolute (U/D≈0.31, Fig. 8) shell with a weakly compressed whorl

section (W/H≈0.62, Fig. 8). The venter is tabulate with angular shoulders and shows a bottleneck shape at the beginning of the flanks. Flanks are longitudinally divided into two parts by a low spiral ridge, which is not apparent on juvenile specimens, and located near the outer third of the flanks. The inner part is flat while the outer part is slightly inclined towards the ventro-lateral shoulder. Umbilicus displays a low vertical wall. Umbilical shoulder is rounded. The ornamentation consists of fine biconcave growth line and weak folds on the flanks. Suture line not preserved.

Material.—Eight specimens from bed GJ-40. Registered specimens: YFMCUG 00085–00089, YFMCUG 00122, YFMCUG 00123-1 and YFMCUG 00127-6.

Remarks.—Ware et al. (in press) provided a detailed review and definition of this species. The rather wide, tabulate venter of our specimens and their evolute shape clearly allow identifying them as *A*. *radiatus*. Comparisons with measurements of Ware et al.'s (in press) specimens highlight this congruence (Fig. 8).

Gyronitidae gen. et sp. indet.

Figure 7.17–7.21

Occurrence.—Lower Daye Formation., Guizhou, South China. *Ophiceras medium* beds, late Griesbachian.

Description.—Small sub-involute (U/D≈0.25), compressed (W/H≈0.46, W/D≈0.26) shell with a tabulate venter and sharp ventro-lateral shoulders. Flanks slightly convex with maximum whorl width near the inner third of the whorl height. Umbilicus moderately deep with a vertical wall, and a rounded umbilical shoulder. Shell surface smooth. The ventral lobe is subdivided into two branches without any indentations visible at their base. The first lateral saddle is broad and shows a rounded tip. The third lateral saddle is relatively small. Only obscure indentations can be seen at the base of the first and second lateral lobe. Auxiliary series not preserved.

Material.—One specimen from bed GJ-15. Registered specimen: YFMCUG 00005.

Remarks.—The tabulate venter and suture line similar to *Gyronites* allow its inclusion in Gyronitidae, and it might correspond to an involute form of the genus. However, only one poorly preserved juvenile specimen is available, so we prefer to keep it in open nomenclature.

?Gyronitidae gen. et sp. indet.

Figures 7.22–7.34, 15.7

Occurrence.—Lower Daye Formation, Guizhou, South China. *Ambites radiatus* bed, middle Dienerian.

Description.—Sub-involute (U/D≈0.23) platyconic shell with a moderately compressed

(W/H≈0.54) whorl section (Fig. 9). Sub-tabulate venter with a distinct rounded ventro-lateral shoulder. Flanks sub-parallel, very slightly convex with maximum whorl width at mid-flank. Umbilicus deep with a vertical wall and a rounded shoulder. Shell with thin, slightly biconcave growth lines crossing the venter. Suture line not preserved.

Material.—Seven specimens from bed GJ-40. Registered specimens: YFMCUG 00094–00098, YFMCUG 00121.

Remarks.—This species differs from Mullericeratidae by a broad sub-tabulate venter and a more evolute and thicker shell. It differs from Proptychitidae by a more compressed shell and sub-tabulate venter. In proptychitids, the venter is always rounded. According to the emended description of Gyronitidae (Ware et al., in press), this species fits within this family. It is quite close to *Ambites bojeseni* (which co-occurs with *Ambites radiatus* in the Northern Indian Margin), differing only by its venter which is not bottleneck-shaped. This difference however excludes it from *Ambites*, so it probably represents a new genus and species within Gyronitidae. However, in the absence of a well-preserved suture line, it is not possible to provide a complete diagnosis, so we prefer to keep it in open nomenclature.

Family Proptychitidae Waagen, 1895

Genus *Jieshaniceras* Brühwiler et al., 2008

Type species.—*Wordieoceras guizhouensis* Zakharov and Mu, 2007 from Guiding, Guizhou,

South China.

Diagnosis.—Compressed and evolute Proptychitidae. Venter rounded without ventro-lateral shoulders. Flanks convex. Suture line with elongated saddles. Lobes with numerous irregular indentations, which typically are positioned along the sides of lobes.

Remarks.—This genus was included in the Flemingitidae by Brühwiler et al. (2008) based on its phylloid saddles. However, Flemingitidae are known to abundantly occur only in the early Smithian (e.g., Brayard and Bucher, 2008; Brühwiler et al., 2012) and are usually distinctly ornamented with ribs and strigation, which is not the case in *Jieshaniceras*. Brühwiler et al. (2008) stated this family assignment remains uncertain. Phylloid saddles also exist in proptychitids (see, e.g., *Proptychites ammonoides* Waagen in Ware et al., in press). Here, our new material with better-preserved suture lines shows that lobe indentations are often not restricted to their base, but also run along the lower part of their sides, particularly on the first lateral lobe (e.g., Figs 10.17 and 12.4). This last trait, together with the rounded venter without ventro-lateral shoulders, is typical of the Proptychitidae (Ware et al., in press). We, therefore, consider here this genus as a compressed and evolute form of Proptychitidae.

Jieshaniceras guizhouense (Zakharov and Mu in Mu et al., 2007)

Figure 10, 11.1–11.6

? 1933 *Meekoceras kweichowense* Tien, p. 16, pl. 2, fig. 1a–e.

? 1988 *Paranorites elegans* Xu, p. 448, pl. 4, figs 4–5.

? 2007 *Proptychites* aff. *candidus*; Zakharov and Mu in Mu et al., p. 864, figs 10.17, 10.18, 11.1.

2007 *Wordieoceras* aff. *wordiei*; Zakharov and Mu in Mu et al., p. 862, figs 6.7, 6.9, 6.11, 7.1, 7.2, 8.

2007 *Wordieoceras guizhouensis* Zakharov and Mu in Mu et al., p. 862, figs 7.3, 9.1, 9.2.

v 2008 *Proptychites candidus*; Brühwiler et al., p. 1162, pl. 2, figs 1–2.

v 2008 *Jieshaniceras guizhouensis*; Brühwiler et al., p. 1174, pl. 6, figs 1–4.

Holotype.—NIGP 140012 (Mu et al., 2007, fig. 9.1–2) from the Wenjiangsi section, Guiding, Guizhou, South China.

Occurrence.—Late Griesbachian of South China.

Description.—Large, moderately evolute (U/D≈0.3) shell with a strongly compressed (W/H≈0.49) whorl section (Fig. 12). Rounded venter lacking ventro-lateral shoulders, and convex flanks with maximum whorl width near mid-flanks. Umbilicus with a low vertical wall and rounded shoulders. Ornamentation not preserved on our specimens. Suture line with high rounded and slightly asymmetric saddles, the first lateral saddle sometimes being phylloid. The third lateral saddle is low and occasionally square (Fig. 11.5). Lobes with numerous deep and irregular indentations. Auxiliary series relatively short with numerous small indentations.

Material.—One specimen from bed GJ-32, one specimen from bed GJ-33, and six specimens from GJ-35. Registered specimens: YFMCUG 00042–00048.

Remarks.—Our specimens fit within the description of the species by Zakharov and Mu in Mu et al. (2007) and Brühwiler et al. (2008). Our specimens are slightly more involute than the holotype (Mu et al., 2007, fig. 9.1–2), have a wider second lateral saddle and more indentations on the lobes, a difference which is interpreted as part of the species' intraspecific variability.

Genus *Proptychites* Waagen, 1895

Type species.—*Ceratites lawrencianus* de Koninck, 1863

Proptychites sp. indet.

Figure 11.7–11.11

Occurrence.—Late Griesbachian of South China.

Description.—Sub-involute (U/D≈0.22) shell with a weakly compressed (W/H≈0.70) whorl section and a broadly rounded venter. Flanks are convex with maximum whorl width near the umbilical shoulder. Umbilicus is deep with an apparently vertical wall and rounded shoulders. The ornamentation is quite obscured on our specimens. Suture line ceratitic, with a broad

ventral lobe divided by a high ventral saddle into two branches with serrated base. The first and second lateral saddles are high and narrow, gently bent towards the umbilicus. The first lateral lobe is larger than the others, with marked denticulations at its base and a couple fine ones on the base of its flanks. Auxiliary series is potentially present but barely visible on our specimens.

Material.—Two specimens from bed GJ-35. Registered specimens: YFMCUG 00049 and YFMCUG 00050.

Remarks.—Our specimens are quite close to *Proptychites lawrencianus*, but their suture line is distinct with a broader first lateral lobe. Saddles of our specimens are also narrower than in *P. lawrencianus.* Compared to *P. candidus*, these specimens show a thicker shell and a broader first lateral lobe. More material is needed to make an unequivocal species assignment.

Genus *Pseudoproptychites* Bando, 1981

Type species.—*Proptychites scheibleri* Diener, 1897

Pseudoproptychites cf. *hiemalis* (Diener, 1895)

Figure 13.1–13.11

? 1895 *Proptychites hiemalis* Diener, p. 34, pl. 2, figs 2, 4, pl. 5, fig. 4.

? 1968 *Proptychites hiemalis*; Zakharov, p. 93, pl. 17, figs 6, 7, text-figure 20c.

v 2008 Proptychitid gen. et sp. indet.; Brühwiler et al., p. 1164, pl. 2, figs 6–8

? 2009 *Pseudoproptychites hiemalis*; Shigeta and Zakharov in Shigeta et al., p. 106, figs 92.7–92.12, 94, 95.

Occurrence.—Middle Dienerian of South China.

Description.—Sub-involute (U/D≈0.25) shell showing a growth allometry. Small individuals display a rounded (W/H≈1.00) whorl section, whereas larger specimens exhibit a moderately compressed (W/H≈0.74) whorl section. The venter is broadly arched without a ventro-lateral shoulder. Flanks highly convex with maximum whorl width at mid-flanks. Umbilicus deep with a vertical wall and a rounded umbilical shoulder. Shell with thin, dense growth lines and a strigation. Suture line not visible on our specimens.

Material.—Four specimens from bed GJ-40. Registered specimens: YFMCUG 00090–00093.

Remarks.—These specimens are quite close to *Pseudoproptychites hiemalis* from South Primorye (Shigeta and Zakharov, 2009). However, this species is poorly known, especially concerning its ontogeny, and our specimens are much smaller than the holotype and do not preserve a suture line, preventing any firm species assignment. Brühwiler et al. (2008) assigned two specimens to Proptychitidae in open nomenclature, which show a similar sub-rounded whorl section and a high expansion rate; these are clearly synonymous with our

specimens.

Family Mullericeratidae Ware et al., 2011

Genus *Mullericeras* Ware et al., 2011

Type species.—*Aspidites spitiensis* Krafft *in* Krafft and Diener, 1909.

Mullericeras gujiaoense new species

Figure 13.12–13.27

vp. 2008 *Koninckites* cf. *timorense*; Brühwiler et al., p. 1165–1166, pl. 3, figs 1, 3, 4

Holotype.—YFMCUG 00018, from bed GJ-33, Guojiao section, Guizhou Province, South China. *Jieshaniceras guizhouense* beds, late Griesbachian.

Diagnosis.—Involute compressed *Mullericeras* with a narrow tabulate venter and slightly convex flanks converging towards the venter. Umbilicus is very small but never occluded. Suture line is typical for *Mullericeras* with a wide ventral lobe with many denticulations at its base and a long auxiliary series characterized by numerous irregular indentations.

Occurrence.—*Jieshaniceras guizhouense* beds, late Griesbachian of Guizhou, South China.

595 *Description*.—Very involute (U/D≈0.13) shell with a strongly compressed (W/H≈0.42) whorl
596 section (Fig. 14). Venter is narrow and tabulate. Flanks convex, converging towards venter.
597 Umbilicus is small and deep with a vertical wall and a rounded umbilical margin. No
598 ornamentation visible on our specimens. Suture line with a broad ventral lobe with numerous
599 irregular indentations, which become larger toward the first lateral saddle. The indentations
600 sometimes go along the side of first lateral saddle. The first and second saddles are narrow
601 and quite high with a narrow rounded tip, the second one being asymmetric. The first lateral
602 lobe is wide with many rather regularly spaced denticulations at its base. The third lateral
603 saddle is small and sometimes with a flattened tip. Auxiliary series very long with numerous
604 irregularly spaced indentations.
605
606 *Etymology*.—Named after Gujiao County.
607
608 *Material*.—Very abundant from bed GJ-33. Registered specimens: YFMCUG 00016–00041.
609
610 *Remarks*.—*Mullericeras* mostly differs from *Ussuridiscus* by a broad ventral lobe bearing
611 numerous small indentations (Ware et al., in press). As our specimens have this feature, we
612 assign them to *Mullericeras*. Our specimens differ from *M. spitiense* and *M. fergusoni* by
613 having a small umbilicus and a narrow tabulate venter, and from *M. shigetai* and *M.*
614 *indusense* by a narrower venter and deeper indentations at the base of the lobes. *M.*
615 *gujiaoense* n. sp. is also more involute than *M. indusense*. It differs from *M. niazii* by a
616 thicker whorl section. *M. gujiaoense* n. sp. occurs in the *Jieshaniceras guizhouense* beds and

617 are thus older than the *Mullericeras* from Candelaria Hills (Ware et al., 2011) and Salt Range
618 (Ware et al., in press), which are all middle Dienerian. In Brühwiler et al. (2008), some
619 specimens identified as *Koninckites* cf. *timorense* from Jieshan Lake, found together with
620 *Jieshaniceras guizhouense* and are of the same age as the present species, are clearly identical
621 to our specimens. The other illustrated specimens they attribute to the same species from
622 Shanggan are younger, from the middle Dienerian (co-occuring with a species synonymized
623 with *Ambites bjerageri*, see Ware et al., in press). They are not well preserved and their suture
624 line is not visible, so it is not possible to decipher whether they are conspecific with our
625 specimens or not, but considering the age difference they likely represent a different species.
626 These smooth, involute, compressed and tabulate Early Triassic forms are very difficult to
627 classify without large populations and good preservation due to frequent homoplasy (see, for
628 example, the similarities between Mullericeratidae, some involute *Ambites*, involute
629 Paranoritidae, some Hedenstroemiidae such as *Clypites* and *Hedenstroemia*, and some
630 Prionitidae such as *Meekoceras*, which are difficult if not impossible to differentiate without
631 large populations and well preserved suture lines). The different Chinese species from Xu
632 (1988) and Mu et al. (2007) Brühwiler et al. (2008) synonymized with it are too poorly
633 preserved for a precise taxonomic assignment.
634
635 Genus *Ussuridiscus* Shigeta and Zakharov, 2009
636
637 *Type species*.—*Meekoceras* (*Kingites*) *varaha* Diener, 1895
638

Ussuridiscus cf. *varaha* Shigeta and Zakharov, 2009

Figure 15.1–15.5, 15.8–15.18

? 2009 *Ussuridiscus varaha*; Shigeta and Zakharov in Shigeta et al., p. 69, figs 50.5–50.6, 55–57.

Occurrence.—Middle Dienerian of South China.

Description.—Involute (U/D≈0.15) shell with a strongly compressed (W/H≈0.43) whorl section (Fig. 16). Tabulate to sub-tabulate venter with a narrowly rounded ventro-lateral shoulder. Flanks are flat from the umbilical shoulder to the middle-flank, and then progressively converge towards ventro-lateral shoulder. Umbilicus very small with a deep vertical wall, and a rounded umbilical shoulder. Fine, dense growth lines are visible, as well as low folds on the outer part of flanks, especially on lager specimens. Suture line poorly preserved in our specimens. Only an auxiliary series is visible and shows a distinct auxiliary lobe and saddle.

Material.—Abundant in bed GJ-40. Registered specimens: YFMCUG 00099–00120, YFMCUG 00123-2, YFMCUG 00124, YFMCUG 00125-1, YFMCUG 00125-2, YFMCUG 00126, YFMCUG 00127-1–00127-5.

Remarks.—Compared with *Ussuridiscus varaha* from South Primorye (Shigeta and Zakharov,

2009) and the Salt Range (Ware et al. in press), our specimens exhibit a tabulate to sub-tabulate venter, which is only visible on larger specimens from South Primorye (see Shigeta and Zakharov, 2009, p. 70, fig. 55, 20–23). In addition, *U. varaha* typically displays an overhanging umbilical wall, whereas our specimens display a vertical one. '*Koninckites*' cf. *timorense* described by Brühwiler et al. (2008), re-assigned to *Ussuridiscus varaha* by Shigeta and Zakharov (2009) and Ware *et al.* (in press) is more depressed than our specimens, and shows converging flanks toward the ventro-lateral shoulders. In contrast, our specimens display relatively flattened flanks. Some specimens of Brühwiler et al. (2008) are clearly synonyms of *Mullericeras gujiaoense* (see above). The suture line is nearly completely obscured on our specimens, but, where visible, exhibits an auxiliary series with a small saddle (Fig. 17). This small saddle was not observed on Shigeta and Zakharov's (2009) specimens. Overall, our specimens superficially resemble *U. varaha* from South Primorye, but exhibit slight differences that may indicate they pertain to another new taxa, but specimens with better-preserved suture lines would be necessary to confirm this.

?Mullericeratidae gen. indet.

Figure 15.19

Occurrence.—Lower Daye Formation, Guizhou, South China. *Ophiceras medium* beds, late Griesbachian.

Description.—Involute (U/D≈0.14) shell with a strongly compressed (W/H≈0.42) whorl

683 section and a tabulate venter with an angular ventro-lateral shoulder. Slightly convex flanks
684 with the maximum whorl width near mid-flank. Umbilicus deep and small with a vertical
685 wall and a rounded shoulder. Shell with very fine growth lines. Suture line not visible.
686
687 *Material*.—Only one poorly preserved specimen from sample GJ-15. Registered specimen:
688 YFMCUG 00004.
689
690 *Remarks*.—The involute shell and tabulate venter of this specimen resemble some
691 Mullericeratidae. This specimen may represent the oldest known occurrence for this family.
692 However, this assignment remains to be confirmed.
693
694 ## Biostratigraphy
695
696 Induan ammonoid faunas and their correlations are still poorly known when compared
697 with Smithian ammonoid faunas (Jenks et al., 2015). The Dienerian ammonoid
698 biostratigraphy has been recently refined by Ware et al. (2015), mainly based on ammonoid
699 data from Salt Range and Spiti. Ware et al. (2015) especially proposed to subdivide the
700 Dienerian into three parts: the early Dienerian corresponding to the first occurrence of the
701 genus *Gyronites* and including three UA-zones (DI-1 to DI-3); the middle Dienerian being
702 based on the occurrence of the genus *Ambites* and comprising five UA-zones (DI-4 to DI-8);.
703 the late Dienerian representing the first occurrences of Paranoritidae and Hedenstroemiidae,
704 and containing four UA-zones (DI-9 to DI-12). However, detailed correlation of this

high-resolution ammonoid zonation with other regions shows many uncertainties (Fig. 18; Jenks et al. 2015). The Griesbachian ammonoid zonation is generally less detailed than for the Dienerian and often shows the successive *Otoceras* and *Ophiceras* Zones (Jenks et al. 2015). *Otoceras* has been found mainly in middle and high latitude regions, thus preventing firm correlation with low latitude regions. *Ophiceras* is much more cosmopolitan and can be considered as a good index of the late Griesbachian (Fig. 18).Intensive sampling of the lower part of Daye Formation, which spans the late Griesbachian–middle Dienerian transition, led to the definition of three successive ammonoid beds. In ascending order, these consist of the late Griesbachian *Ophiceras medium* and *Jieshaniceras guizhouense* beds followed by the middle Dienerian *Ambites radiatus* bed (Figs 3, 18). Typical early Dienerian faunas are thus absent from the Gujiao section. Owing to a preservation gap, no ammonoid specimen was found between *Jieshaniceras guizhouense* beds and *Ambites radiatus* bed. Abundant bivalves (e.g., *Claraia radialis*, *C. stachei*, and *C. aurita*) were found in *Jieshaniceras guizhouense* beds and *Ambites radiatus* bed, also indicating a Griesbachian–Dienerian age for these beds.Ophiceras medium *beds*.—These beds are characterized by the occurrence of *Ophiceras medium*. Other co-occurring taxa are ?Mullericeratidae gen. indet, Gyronitidae gen. indet., *Vishnuites pralambha* and Ophiceratidae gen. indet. This assemblage indicates a late Griesbachian age. *Ophiceras* or *Ophiceras-Lytophiceras* zones have been reported from many areas of South China, for instance the Meishan section in Zhejiang Province (Wang, 1984; Yin et al., 2001), the Qinglongshan section in Jiangsu Province (Wang, 1984), and the Chaohu section in Anhui Province (Tong and Wu, 2004). However, most illustrated specimens from these sections are poorly preserved, preventing any firm taxonomic

assignment and correlation among sections. Brühwiler et al. (2008) also recognized *Ophiceras* sp. indet. from the Laren and Shanggan sections in Guangxi. *Ophiceras* is a widely distributed Griesbachian genus and has been documented in the Himalayas (e.g., Diener, 1897; Krystyn and Orchard, 1996; Wang and He, 1976), in East Greenland (Spath, 1930; 1935; Trümpy, 1969), in Arctic Canada (Tozer, 1994), in Oman (Krystyn et al., 2003), in the Salt Range (Schindewolf, 1954; Kummel, 1966; Ware et al., in press) and in South China (Tien, 1933; Tong and Wu., 2004; Brühwiler et al., 2008), permitting worldwide correlation among "*Ophiceras* beds", but their temporal resolution and potential subdivisions remain to be analyzed in depth.

Jieshaniceras guizhouense *beds*.—These beds contain *Jieshaniceras guizhouense*, *Proptychites* sp. indet., *Mullericeras gujiaoense* n. sp., *Ophiceras* sp. indet. and *Vishnuites pralambha*. *Jieshaniceras guizhouense* is associated with *Ussuridiscus varaha* in some sections (e.g., Jieshan Lake and Jianzishan, Brühwiler et al., 2008; Bai et al., 2017). The age assignment of these beds, if based exclusively on ammonoids, remains problematic. *U. varaha* was found restricted to the first Dienerian zone of the Northern Indian Margin (Ware et al., in press), but its occurrence in South Primorye is less effectively constrained and assigned to the late Griesbachian through to the middle Dienerian (Shigeta and Zakharov, 2009). Use of this taxon for biostratigraphic correlation thus does not bring much clarity. Proptychitids occur from the latest Griesbachian to the Smithian and do not provide any useful biostratigraphic information. *Ophiceras* together with *Otoceras* represent iconic Griesbachian genera and has yet to be found in younger strata, suggesting a Griesbachian age. However, *Mullericeras* is only known in the middle Dienerian of South Primorye

(Shigeta and Zakharov, 2009), Nevada (Ware et al., 2011) and Northern Indian Margin (Ware et al., 2015, in press), so its occurrence in these beds suggests a Dienerian age instead. This assemblage was found in Jieshan Lake by Brühwiler et al. (2008), who considered it as a direct correlative of the Dienerian *Proptychites candidus* beds of Tozer (1994), but Mu et al. (2007) considered the same assemblage in Wenjiangsi as late Griesbachian in age. Overall, the ammonoid assemblage found in the *J. guizhouense* beds at Gujiao shows that our knowledge on the temporal distribution of several Induan ammonoid taxa, especially around the Griesbachian/Dienerian boundary, remains unclear, making the Griesbachian/Dienerian boundary hard to determine based on ammonoid faunas only.

Conodonts show an important turnover at this boundary, with the replacement of anchignathodids by neospathodids and other segminate conodonts (Orchard, 2007; Brosse et al., 2017). Mu et al. (2007) reported some typically Griesbachian conodonts such as *Neogondolella krystyni* and *N. carinata* in Wenjiangsi. Samples from the same beds where Brühwiler et al. (2008) found *Jieshaniceras guizhouense* also contain some neogondolellids and *Hindeodus parvus* (N. Goudemand, comm. pers. 2017). In addition, Bai et al. (2017) reported several species of *Hindeodus* in the *Jieshaniceras guizhouense* beds and slightly higher up in the Jianzishan section. Using this conodont turnover as a proxy for the Griesbachian/Dienerian boundary, the *Jieshaniceras guizhouense* beds are therefore clearly late Griesbachian in age, and represent the oldest occurrence of the genus *Mullericeras*.

Ambites radiatus *bed*.—This bed yields *Ambites radiatus*, *Ussuridiscus* cf. *varaha*, ?Gyronitidae gen. et sp. indet., and *Pseudoproptychites* cf. *hiemalis*. This assemblage

771 is middle Dienerian in age and can be directly correlated with the UA-zone DI-5 from Salt
772 Range and Spiti (Ware et al., 2015). It also roughly corresponds to the *Ambitoides fuliginatus*
773 Zone in South Primorye (Shigeta and Zakharov, 2009), based on the occurrence of
774 *Ussuridiscus*. However, *Ussuridiscus* is a long-ranging genus and the assignment of our
775 specimens to *Ussuridiscus varaha* remains to be firmly confirmed . Additional well-preserved
776 material is therefore needed to verify this correlation. The *Proptychites candidus* Zone in
777 Arctic Canada contains several forms of *Ambites*, which is the index of middle Dienerian
778 (Tozer, 1994; Ware et al., 2015), thus it can be roughly correlated with *Ambites radiatus* bed
779 at Gujiao.
780

781 ## Diversity pattern

782

783 Ammonoids almost went extinct during the Permian-Triassic mass extinction, but their
784 rediversification during the Early Triassic was extremely rapid, reaching in less than 1 myr
785 (i.e., during the Smithian) diversity levels higher than during the Permian (Brayard et al.,
786 2009). This nondelayed recovery after the PT mass extinction probably results from intrinsic
787 ammonoid parameters related for instance to their high evolutionary rates (e.g., Brayard et al.,
788 2009; Stanley, 2009; Brühwiler et al. 2010), dispersal abilities (e.g., Brayard et al. 2006, 2007)
789 and positions in trophic webs (e.g., Brayard et al., 2009). First ammonoids found in the
790 Griesbachian often show rather cosmopolitan distributions (e.g., Brayard et al., 2007, 2009)
791 suggesting that they were rather generalist organisms at that time. This may agree with
792 hypotheses of Kauffman and Harries (1996), Harries et al. (1996) and Bambach (2002)

suggesting that some surviving organisms were favored after mass extinctions if generalist and motile. However, this configuration rapidly shifted from the Dienerian up to the Spathian towards more and more endemic genera; this was possibly related to successive changes in Ocean temperature and chemistry and highlight that Early Triassic ammonoids become highly sensitive organisms to environmental fluctuations during this time interval (e.g., Brosse et al. 2013; Romano et al. 2013; Ware et al., 2015; Jattiot et al. 2016).

Only three different surviving ammonoid lineages survived the PT mass extinction and pertain to Episageceratidae, Xenodiscaceae and Otoceratacеae (e.g., Brayard et al., 2007; Brayard and Bucher, 2015). Early Triassic Episageceratidae are represented by a single genus: *Episageceras*. This taxon is rare and documented mainly from Himalaya and Russia (Diener, 1897; Zakharov, 1978). Only two genera, *Otoceras* and *Proharpoceras*, derived from Otoceratacеae have been documented from the Griesbachian and Smithian, respectively(e.g., Brayard et al., 2007; Brühwiler et al., 2012; Jenks and Brayard, 2018). It is thus commonly accepted that all other Triassic Ceratitids root in Xenodiscaceae (e.g., Brayard et al., 2006; Zakharov and Popov, 2014). However, many uncertainties remain about the exact phylogeny of Early Triassic ammonoids. For instance, whether Proptychitidae are derived from Ophiceratidae or Otoceratidae remains an open question (Zakharov, 2002; Ware et al., in press). In total, 13 ammonoid species have been recognized in the Induan of Gujiao (Fig. 3). Five species are identified in the *Ophiceras medium* beds, five species in the *Jieshaniceras guizhouense* beds and four species in the *Ambites radiatus* bed. The apparent absence of typical early Dienerian ammonoids may result from local environmental change or taphonomic conditions, while no distinct unconformity or facies change was observed in the

field from upper Griesbachian to middle Dienerian.

Although our data are scarcer than in the Northern Indian Margin (NIM), ammonoid diversity patterns appear relatively congruent, especially when combined to data from previous publications on Early Triassic Chinese ammonoids (e.g., Brayard and Bucher, 2008; Brühwiler et al., 2008). NIM diversity pattern shows a maximum species richness during the early Dienerian followed by low values during the middle–late Dienerian and a marked diversification after the Dienerian/Smithian boundary (Brühwiler et al., 2010; Ware et al., 2015). The Chinese ammonoid diversity fluctuations resemble the ones observed for the NIM. However, the sampled species richness in South China is apparently lower than in the NIM, which shows 47 species for the Dienerian (Ware et al., 2015). Therefore, some uncertainties on regional diversity patterns remain and potentially result from preservational and sample biases in South China. The Griesbachian–Dienerian ammonoid fauna remains quite scattered and rare.

Additionally, the Induan (Griesbachian and Dienerian) and early Smithian ammonoid diversity fluctuations may be closely related to local oceanic redox conditions. Recent analysis of the size distribution of pyrite framboids at Gujiao indicates that the late Griesbachian *Ophiceras medium* beds and *Jieshaniceras guizhouense* beds were probably oxic (Dai et al., in review). This hypothesis is also supported by the relatively high abundance of ichnofossils, e.g., *Arenicolites*. Using the same indicators, the *Ambites radiatus* bed and overlying beds were probably dysoxic or anoxic. Therefore, the observed low taxonomic richness is concomitant with the potentially more dysoxic/anoxic conditions. A similar trend has been observed on the Northern Indian Margin (Hermann et al., 2011; Ware et al., 2015).

Similar relatively high diversity levels in ameliorated environments occur in other locations of South China during the late Griesbachian–early Dienerian (Xu, 1988; Song et al., 2012; Tian et al., 2014; Wang et al., 2017). Relatively high taxonomic richness for the same time interval are also reported from other regions, such as the western USA (Hofmann et al., 2013) and Oman (Krystyn et al., 2003). This supports the hypothesis of a first diversification phase during the late Griesbachian–early Dienerian when deleterious environmental conditions potentially decreased or ceased after the Permian–Triassic mass extinction. However, the accurate spatio-temporal extent of such diversity pattern, as well as its underlying processes, remains to be determined.

Conclusions

1. Three different Induan ammonoid faunas occur at Gujiao, consisting of eight identified genera and 13 species, including one new species: *Mullericeras gujiaoense* n. sp.
2. Three successive ammonoid zones were identified: the late Griesbachian *Ophiceras medium* beds and *Jieshaniceras guizhouense* beds, and the middle Dienerian *Ambites radiatus* bed.
3. Integrated with data from previous publications on Early Triassic Chinese ammonoids, our data suggest that the regional Induan taxonomic richness trend rather resembles the one identified from the extensively sampled of the Northern Indian Margin, indicating that this signal is probably global. High and low ammonoid richness levels, respectively in the late Griesbachian and in the middle Dienerian, can be identified at Gujiao.

Acknowledgments

We thank J. Chen, X. Xiong, Y. Zhao, X. Sun, S. Jiang, E. Jia, J. Yan, F. Wang, X. Liu, K. Wang and R. Bai for their help on the field. This study is supported by the National Natural Science Foundation of China (41622207, 41530104, 41661134047), and the 111 Project (B08030). This is a contribution to the ANR project AFTER (ANR-13-JS06-0001-01; to A.B.) and to the IGCP-630.

References

Algeo, T.J., and Twitchett, R.J, 2010, Anomalous Early Triassic sediment fluxes due to elevated weathering rates and their biological consequences: Geology, v. 38, p. 102–1026.

Arthaber, G, 1911, Die Trias von Albanien: Beiträge zur Paläontologie und Geologie Österreich-Ungarns und des Orients, v. 24, p. 169–277.

Bagherpour, B., Bucher, H., Baud, A., Brosse, M., Vennemann, T., Martini, R., and Guodun, K., 2017, Onset, development, and cessation of basal Early Triassic microbialites (BETM) in the Nanpanjiang pull-apart Basin, South China Block: Gondwana Research, v. 44, p. 178–204.

Bai, R., Dai, X., and Song, H., 2017, Conodont and ammonoid biostratigraphies around Permian-Triassic boundary from Jianzishan of Hubei, South China: Journal of Earth Science, v. 28, p. 595–613.

881 Bando, Y., 1981. Lower Triassic ammonoids from Guryul Ravine and the Spur three
882 kilometers north of Burus. *In* K. Nakazawa and H. M. Kapoor (eds.), The Upper
883 Permian and Lower Triassic fossils of Kashmir: Palaeontologia Indica, New Series 46,
884 p. 137–171.
885 Baresel, B., Bucher, H., Brosse, M., Cordey, F., Guodun, K., and Schaltegger, U., 2017,
886 Precise age for the Permian-Triassic boundary in South China from high-precision U-Pb
887 geochronology and Bayesian age-depth modeling: Solid Earth, v. 8, p. 361–378.
888 Bengtson, P., 1988, Open nomenclature: Palaeontology, v. 31, p. 223–227.
889 Brayard, A., Bucher, H., Bruehwiler, T., Galfetti, T., Goudemand, N., Guodun, K., Escarguel,
890 G., and Jenks, J., 2007, *Proharpoceras* Chao: a new ammonoid lineage surviving the
891 end-Permian mass extinction: Lethaia, v. 40, no. 2, p. 175–181.
892 Brayard, A., and Bucher, H., 2008, Smithian (Early Triassic) ammonoid faunas from
893 northwestern Guangxi (South China): taxonomy and biochronology: Fossils and Strata,
894 v. 55, p. 1–184.
895 Brayard, A., Bucher, H., Escarguel, G., Fluteau, F., Bourquin, S., and Galfetti, T., 2006, The
896 Early Triassic ammonoid recovery: paleoclimatic significance of diversity
897 gradients: Palaeogeography, Palaeoclimatology, Palaeoecology, v. 239, p. 374–395.
898 Brayard, A., Escarguel, G., Bucher, H., Monnet, C., Brühwiler, T., Goudemand, N., Galfetti,
899 T., and Guex, J., 2009, Good genes and good luck: ammonoid diversity and the
900 end-Permian mass extinction: Science, v. 325, p. 1118–1121.
901 Brosse, M., Baud, A., Bhat, G.M., Bucher, B., Leu, M., Vennemann, T., and Goudemand, N.,
902 Conodont-based Griesbachian biochronology of the Guryul Ravine section (basal

903 Triassic, Kashmir, India): Geobios, v. 50, no. 5–6, p. 359–387.
904 Brosse, M., Bucher, H., Bagherpour, B., Baud, A., Frisk, Å. M., Guodun, K., and Goudemand,
905 N., 2015, Conodonts from the Early Triassic microbialite of Guangxi (South China):
906 implications for the definition of the base of the Triassic System: Palaeontology, v. 58,
907 no. 3, p. 563–584.
908 Brosse, M., Bucher, H., and Goudemand, N., 2016, Quantitative biochronology of the
909 Permian–Triassic boundary in South China based on conodont unitary
910 associations: Earth-Science Reviews, v. 155, p. 153–171.
911 Brühwiler, T., Brayard, A., Bucher, H., and Guodun, K., 2008, Griesbachian and Dienerian
912 (Early Triassic) ammonoid faunas from Northwestern Guangxi and Southern Guizhou
913 (South China): Palaeontology, v. 51, p. 1151–1180.
914 Brühwiler, T., Bucher, H. Brayard, A., and Goudemand, N., 2010, High-resolution
915 biochronology and diversity dynamics of the Early Triassic ammonoid recovery: The
916 Smithian faunas from the North Indian Margin: Palaeogeography, Palaeoclimatology,
917 Palaeoecology, v. 297, p. 491–501.
918 Brühwiler, T., Bucher, H., Roohi, G., Yaseen, A., and Rehman, K., 2011, A new early
919 Smithian ammonoid fauna from the Salt Range (Pakistan): Swiss Journal of
920 Palaeontology, v. 130, p. 187–201.
921 Brühwiler, T., Bucher, H., Ware, D., Hermann, E., Hochuli, P. A., Roohi, G., Rehman, K., and
922 Yaseen, A., 2012, Smithian (Early Triassic) ammonoids from the Salt Range, Pakistan:
923 Special papers in Palaeontology, v. 88, p. 1–114.
924 Brühwiler, T., Ware, D., Bucher, H., Krystyn, L., and Goudemand, N., 2010, New Early

925 Triassic ammonoid faunas from the Dienerian/Smithian boundary beds at the
926 Induan/Olenekian GSSP candidate at Mud (Spiti, Northern India): Journal of Asian
927 Earth Sciences, v. 39, p. 724–739.
928 Bu, J., Wu, S., Zhang, H., Meng, Y., Zhang, F., and Zhang, L., 2006, Permian-Triassic
929 cephalopods from Dongpan Section, Guangxi, and its geological significance:
930 Geological Science and Technology Information, v. 25, p. 47–51.
931 Chao, K., 1959, Lower Triassic ammonoids from Western Kwangsi, China: Palaeontologia
932 Sinica New Series B, v. 9, p. 1–355, pls 1–45.
933 Chen, J., Tong, J., Song, H., Luo, M., Huang, Y., and Xiang, Y., 2015, Recovery pattern of
934 brachiopods after the Permian-Triassic crisis in South China: Palaeogeography,
935 Palaeoclimatology, Palaeoecology, v. 433, p. 91–105.
936 Chen, Z.Q., and Benton, M.J., 2012, The timing and pattern of biotic recovery following the
937 end-Permian mass extinction: Nature Geoscience, v. 5, p. 375–383.
938 Clarkson, M., Kasemann, S., Wood, R., Lenton, T., Daines, S., Richoz, S., Ohnemueller, F.,
939 Meixner, A., Poulton, S., and Tipper, E., 2015, Ocean acidification and the
940 Permo-Triassic mass extinction: Science, v. 348, p. 229–232.
941 de Koninck, L.G., 1863, Description of some fossils from India, discovered by Dr. A.
942 Fleming, of Edingburgh: The Quarterly Journal of the Geological Society of London, v.
943 19, p. 1–19.
944 Diener, C., 1895, Triadische Cephalopodenfaunen der ostsibirischen Küstenprovinz:
945 Mémoires du Comité Géologique St Petersburg, v. 14, 59 p.
946 Diener, C., 1897, The Cephalopoda of the Lower Trias: Palaeontologia Indica, v. 15, 181 p.

947 Diener, C., 1913, Triassic faunae of Kashmir: Palaeontologia Indica, v. 5, 133 p.
948 Feng, Z., Bao, Z., and Liu, S., 1997, Lithofacies palaeogeography of Early and Middle
949 Triassic of South China: Beijing, Petroleum Industry Press, 222 p.
950 Foster, W.J., Danise, S., Price, G.D., and Twitchett, R.J., 2017, Subsequent biotic crises
951 delayed marine recovery following the late Permian mass extinction event in northern
952 Italy: PLoS One, v. 12, p. e0172321.
953 Galfetti, T., Bucher, H., Martini, R., Hochuli, P.A., Weissert, H., Crasquin-Soleau, S.,
954 Brayard, A., Goudemand, N., Brühwiler, T., and Guodun, K., 2008, Evolution of Early
955 Triassic outer platform paleoenvironments in the Nanpanjiang Basin (South China) and
956 their significance for the biotic recovery: Sedimentary Geology, v. 204, p. 36–60.
957 Galfetti, T., Bucher, H., Ovtcharova, M., Schaltegger, U., Brayard, A., Brühwiler, T.,
958 Goudemand, N., Weissert, H., Hochuli, P.A., Cordey, F., and Guodun, K., 2007, Timing
959 of the Early Triassic carbon cycle perturbations inferred from new U–Pb ages and
960 ammonoid biochronozones: Earth and Planetary Science Letters, v. 25, p. 593–604.
961 Griesbach, C.L., 1880, Palaeontological notes on the Lower Trias of the Himalayas: Records
962 of the Geological Survey of India, v. 13, no. 2, p. 94–113.
963 Hallam, A., 1991, Why was there a delayed radiation after the end−Palaeozoic extinctions?:
964 Historical Biology, v. 5, p. 257–262.
965 Harries, P. J., Kauffman, E. G., and Hansen, T. A., 1996, Models for biotic survival following
966 mass extinction: Geological Society, London, Special Publications, v. 102, no. 1, p.
967 41–60.
968 Harries, P.J., and Knorr, P.O., 2009, What does the 'Lilliput Effect'mean?: Palaeogeography,

969 Palaeoclimatology, Palaeoecology, v. 284, no. 1–2, p. 4–10.
970 Hermann, E., Hochuli, P.A., Méhay, S., BuYincher, H., Brühwiler, T., Ware, D., Hautmann,
971 M., Roohi, G., ur-Rehman, K., and Yaseen, A., 2011, Organic matter and
972 palaeoenvironmental signals during the Early Triassic biotic recovery: The Salt Range
973 and Surghar Range records: Sedimentary Geology, v. 234, p. 19–41.
974 Hsü, T.Y., 1937, Contribution to the marine Lower Triassic fauna of Southern China: Bulletin
975 of the Geological Society of China, v. 16, p. 303–347.
976 Huang, Y., Tong, J., Fraiser, M.L., and Chen, Z., 2014, Extinction patterns among bivalves in
977 South China during the Permian-Triassic crisis: Palaeogeography, Palaeoclimatology,
978 Palaeoecology, v. 399, p. 78–88.
979 Hyatt, A., 1884, Genera of fossil cephalopods: Proceedings of the Boston Society of Natural
980 History, v. 22, p. 253–338.
981 Jattiot, R., Bucher, H., Brayard, A., Brosse, M., Jenks, J., and Bylund, K.G, 2017, Smithian
982 ammonoid faunas from northeastern Nevada: implications for Early Triassic
983 biostratigraphy and correlation within the western USA basin: Palaeontographica
984 Abteilung A, v. 309, p. 1–89.
985 Jenks, J.F., Monnet, C., Balini, M., Brayard, A., and Meier, M., 2015, Biostratigraphy of
986 Triassic ammonoids. In: Klug, C., et al. (Eds.), Ammonoid Paleobiology: from
987 macroevolution to paleogeography: Top. Geobiol. 44. Springer, New York, p. 329–388.
988 Jiang, H., Lai, X., Sun, Y., Wignall, P.B., Liu, J., and Yan, C., 2014, Permian-Triassic
989 conodonts from Dajiang (Guizhou, South China) and their implication for the age of
990 microbialite deposition in the aftermath of the end-Permian mass extinction: Journal of

991 Earth Science, v. 25, p. 413–430.
992 Joachimski, M. M., Lai, X., Shen, S., Jiang, H., Luo, G., Chen, B., Chen, J., and Sun, Y.,
993 2012, Climate warming in the latest Permian and the Permian-Triassic mass extinction:
994 Geology, v. 40, p. 195–198.
995 Kaim, A., Nützel, A., Bucher, H., Brühwiler, T., and Goudemand, N, 2010, Early Triassic
996 (Late Griesbachian) gastropods from South China (Shanggan, Guangxi): Swiss Journal
997 of Geosciences, v. 103, p. 121–128.
998 Kauffman, E.G., and Harries, P.J., 1996, The importance of crisis progenitors in recovery
999 from mass extinction: Geological Society, London, Special Publications, v. 102, no. 1, p.
1000 15–39.
1001 Krafft, A.V., and Diener, C., 1909, Lower Triassic cephalopoda from Spiti, Malla Johar, and
1002 Byans: Palaeontologia Indica, v. 15, 186 p.
1003 Krystyn, L., Balini, M. & Nicora, A. 2004. Lower and Middle Triassic stage and substage
1004 boundaries in Spiti. Albertiana, 3: 40-53.
1005 Krystyn, L., and Orchard, M.J., 1996, Lowermost Triassic ammonoid and conodont
1006 biostratigraphy of Spiti, India: Albertiana, v. 17, p. 10–21.
1007 Krystyn, L., Richoz, S., Baud, A., and Twitchett, R.J., 2003, A unique Permian-Triassic
1008 boundary section from the Neotethyan Hawasina Basin, Central Oman Mountains:
1009 Palaeogeography, Palaeoclimatology, Palaeoecology, v. 191, p. 329–344.
1010 Krystyn, L., Richoz, S., and Bhargava, O.N., 2007, The Induan-Olenekian Boundary (IOB) in
1011 Mud—an update of the candidate GSSP section M04: Albertiana, v. 36, p. 33–45.
1012 Kummel, B., 1966, The Lower Triassic Formations of the Salt Range and Trans-Indus Ranges,

West Pakistan: Bulletin of the Museum of Comparative Zoology, v. 134, p. 361-429.

Kummel, B., 1972, The Lower Triassic (Scythian) ammonoid *Octoceras*: Bulletin Museum Comparative Zoology, v. 143, p. 365–393

Lehrmann, D. J., Wei, J., and Enos, P., 1998, Controls on facies architecture of a large Triassic carbonate platform: the Great Bank of Guizhou, Nanpanjiang Basin, South China: Journal of Sedimentary Research, v. 68, p. 311–326.

Liang, L., Tong, J., Song, H., Song, T., Tian, L., Song, H., and Qiu, H., 2016, Lower-Middle Triassic conodont biostratigraphy of the Mingtang section, Nanpanjiang Basin, South Chin: Palaeogeography, Palaeoclimatology, Palaeoecology, v. 459, p. 381–393.

Matthews, S.C., 1973, Notes on open nomenclature and synonymy lists: Palaeontology, v. 16, p. 713–719.

Mu, L., Zakharov, Y., Li, W., and Shen, S., 2007, Early Induan (Early Triassic) cephalopods from the Daye Formation at Guiding, Guizhou Province, South China: Journal of Paleontology, v. 81, p. 858–872.

Oppel, A., 1865, Ueber ostindische Fossilrest (Fortsetzung): Palaeontologische Mittheilungen aus dem Museum Des Koeniglich-Bayerischen Staates 4, p. 289–304.

Orchard, M.J., 2007, Conodont diversity and evolution through the latest Permian and Early Triassic upheavals: Palaeogeography, Palaeoclimatology, Palaeoecology, v. 252, p. 93-117.

Pan, H.Z., Erwin, D.H., Nützel, A., and Zhu, X.S., 2003, *Jiangxispira*, a new gastropod genus from the Early Triassic of China with remarks on the phylogeny of the Heterostropha at the Permian/Triassic boundary: Journal of Paleontology, v. 77, p. 44–49.

1035 Payne, J.L., Lehrmann, D.J., Wei, J., Orchard, M.J., Schrag, D.P., and Knoll, A.H., 2004,
1036 Large perturbations of the carbon cycle during recovery from the end-Permian
1037 extinction: Science, v. 305, p. 506–509.
1038 Raup, D.M., 1979, Size of the Permo-Triassic bottleneck and its evolutionary implications:
1039 Science, v. 206, p. 217–218.
1040 Romano, C., Goudemand, N., Vennemann, T.W., Ware, D., Schneebeli-Hermann, E., Hochuli,
1041 P.A., Brühwiler, T., Brinkmann, W., and Bucher, H., 2012, Climatic and biotic upheavals
1042 following the end-Permian mass extinctio: Nature Geoscience, v. 6, p. 57–60.
1043 Schindewolf, O.H., 1954, Über die Faunenwende vom Paläozoikum zum Mesozoikum:
1044 Zeitschrift der Deutschen Geologischen Gesellschaft, v. 105, p. 153-182.
1045 Scotese, C.R., 2001, Atlas of earth history: University of Texas at Arlington. Department of
1046 Geology. PALEOMAP Project.
1047 Shigeta, S., Zakharov, Y.D., 2009. Cephalopods. In: Shigeta, Y., Zakharov, Y.D., Maeda, H.,
1048 Popov, A.M. (Eds.), The Lower Triassic System in the Abrek Bay Area, South Primorye,
1049 Russia: National Museum of Nature and Science Monographs, v. 38, p. 44–140.
1050 Song, H., Jiang, G., Poulton, S. W., Wignall, P. B., Tong, J., Song, H., An, Z., Chu, D., Tian,
1051 L., She, Z., and Wang, C., 2017, The onset of widespread marine red beds and the
1052 evolution of ferruginous oceans: Nature Communications, v. 8, p. 399.
1053 Song, H., Wignall, P.B., Chen, Z., Tong, J., Bond, D.P., Lai, X., Zhao, X., Jiang, H., Yan, C.,
1054 and Niu, Z., 2011, Recovery tempo and pattern of marine ecosystems after the
1055 end-Permian mass extinction: Geology, v. 39, p. 739–742.
1056 Song, H., Wignall, P.B., Tong, J., Bond, D.P., Song, H., Lai, X., Zhang, K., Wang, H., and

1057 Chen, Y., 2012, Geochemical evidence from bio-apatite for multiple oceanic anoxic
1058 events during Permian-Triassic transition and the link with end-Permian extinction and
1059 recovery: Earth and Planetary Science Letters, v. 353, p. 12–21.
1060 Song, H., Wignall, P.B., Tong, J., Song, H., Chen, J., Chu, D., Tian, L., Luo, M., Zong, K.,
1061 Chen, Y., Lai, X., Zhang, K., an Wang, H., 2015a, Integrated Sr isotope variations and
1062 global environmental changes through the Late Permian to early Late Triassic: Earth and
1063 Planetary Science Letters, v. 424, p. 140–147.
1064 Song, H., Wignall, P.B., Tong, J., and Yin, H., 2013, Two pulses of extinction during the
1065 Permian-Triassic crisis: Nature Geoscience, v. 6, p. 52–56.
1066 Song, H., Yang, L., Tong, J., Chen, J., Tian, L., Song, H., and Chu, D., 2015b, Recovery
1067 dynamics of foraminifers and algae following the Permian-Triassic extinction in
1068 Qingyan, South China: Geobios, v. 48, p. 71–83.
1069 Spath, L.F., 1930, The Eo-Triassic invertebrate fauna of East Greenland: Meddelelser om
1070 Grønland, v. 83, 90 p. 12 pls.
1071 Spath, L.F., 1934, Catalogue of the Fossil Cephalopoda in the British Museum (Natural
1072 History). The ammonoidea of the Trias: The Trustees of the British Museum, London,
1073 521 p. 18 pls.
1074 Spath, L.F., 1935, Additions to the Eo-Triassic invertebrate fauna of East Greenland:
1075 Meddelelser om Grønland, v. 98, 115 p. 23 pls.
1076 Stanley, S.M. 2016, Estimates of the magnitudes of major marine mass extinctions in earth
1077 history: Proceedings of the National Academy of Sciences, v. 113, no. 42, p.
1078 E6325–E6334, doi:10.1073/pnas.1613094113.

1079 Sun, Y., Joachimski, M.M., Wignall, P.B., Yan, C., Chen, Y., Jiang, H., Wang, L., and Lai, X.,
1080 2012, Lethally hot temperatures during the Early Triassic greenhouse: Science, v. 338, p.
1081 366–370.
1082 Tian, L., Tong, J., Algeo, T.J., Song, H., Song, H., Chu, D., Shi, L., and Bottjer, D.J., 2014,
1083 Reconstruction of Early Triassic ocean redox conditions based on framboidal pyrite
1084 from the Nanpanjiang Basin, South China: Palaeogeography, Palaeoclimatology,
1085 Palaeoecology, v. 412, p. 68–79.
1086 Tien, C.C., 1933, Lower Triassic cephalopods of South China: Palaeontologia Sinica, Series
1087 B, v. 15, 53 p.
1088 Tong, J., and Wu, S., 2004, Early Triassic ammonoid succession in Chaohu, Anhui Province:
1089 Acta Palaeontologica Sinica, v. 43, p. 192–204.
1090 Tong, J., Zhang, S., Zuo, J., and Xiong, X., 2007, Events during Early Triassic recovery from
1091 the end-Permian extinction: Global and Planetary Change, v. 55, p. 66–80.
1092 Tozer, E.T., 1961, Triassic stratigraphy and faunas, Queen Elizabeth Islands, Arctic
1093 Archipelago: Memoirs of the Geological Survey of Canada, v. 316, 116 p.
1094 Tozer, E.T., 1994, Canadian Triassic ammonoid faunas: Geological Survey of Canada, v. 467,
1095 663 p.
1096 Trümpy, R., 1969, Lower Triassic ammonites from Jameson Land (East Greenland):
1097 Meddelelser om Grønland, v. 168, p. 77–116.
1098 Twitchett, R.J., Krystyn, L., Baud, A., Wheeley, J.R., and Richoz, S., 2004, Rapid marine
1099 recovery after the end-Permian mass-extinction event in the absence of marine anoxia:
1100 Geology, v. 32, p. 805–808.

1101 Waagen, W.H., 1895, Salt-Range Fossils. Vol. 2: fossils from the Ceratite Formation:
1102 Palaeontologia Indica, v. 13, 323 p. 40 pls.
1103 Wang, F., Chen, J., Dai, X., and Song, H., 2017, A new Dienerian (Early Triassic) brachiopod
1104 fauna from South China and implications for biotic recovery after the Permian-Triassic
1105 extinction: Papers in Palaeontology, v. 3, p. 425–439.
1106 Wang, Y., 1984, Earliest Triassic ammonoid faunas from Jiangsu and Zhejiang and their
1107 bearing on the definition of Permo-Triassic boundary: Acta Palaeontologica Sinica, v.
1108 23, p. 257–269.
1109 Wang, Y., and He, G., 1976, Triassic ammonoids from the Mount Jolmo Lungma region: A
1110 report of scientific expedition in the Mount JolmoLungma region (1966-1968),
1111 Palaeontology 3, p. 223–502.
1112 Ware, D., Bucher, H., Brayard, A., Schneebeli-Hermann, E., and Brühwiler, T., 2015,
1113 High-resolution biochronology and diversity dynamics of the Early Triassic ammonoid
1114 recovery: The Dienerian faunas of the Northern Indian Margin: Palaeogeography,
1115 Palaeoclimatology, Palaeoecology, v. 440, p. 363–373.
1116 Ware, D., Bucher, H., Brühwiler, T., Schneebeli-Hermann, E., Hochuli, P.A., Roohi, G.,
1117 Ur-Rehman, K., and Yaseen, A., 2017, Griesbachian and Dienerian (Early Triassic)
1118 ammonoids from the Salt Range, Pakistan: Fossils and Strata (in press).
1119 Ware, D., Jenks, J.F., Hautmann, M., and Bucher, H., 2011, Dienerian (Early Triassic)
1120 ammonoids from the Candelaria Hills (Nevada, USA) and their significance for
1121 palaeobiogeography and palaeoceanography: Swiss Journal of Geosciences, v. 104, p.
1122 161–181.

1123 Wignall, P. B., and Twitchett, R.J., 1996, Oceanic anoxia and the end Permian mass
1124 extinction: Science, v. 227, p. 1155–1158.
1125 Xu, G., 1988, Early Triassic cephalopods from Lichuan, Western Hubei: Acta Palaeontologica
1126 Sinica, v. 27, p. 437–456.
1127 Yin, H., 1985, Bivalves near the Permian-Triassic Boundary in South China: Journal of
1128 Paleontology, v. 5, p. 572–600.
1129 Yin, H., Zhang, K., Tong, J., Yang, Z. and Wu, S. 2001. The global stratotype section and
1130 point (GSSP) of the Permian-Triassic boundary: Episodes, v. 24, p. 102–114.
1131 Zakharov, Y.D, 1968, Lower Triassic Biostratigraphy and Ammonoids of South Primorye:
1132 Nauka, Moskva, 172 p.
1133 Zakharov, Y.D., 1978, Lower Triassic Ammonoids of East USSR: Nauka, Moskva, 224 p.
1134 Zakharov, Y.D, 1997, Recent view on the Induan, Olenekian and Anisian ammonoid taxa and
1135 zonal assemblages of South Primorye: Albertiana, v. 19, p. 25–35.
1136 Zakharov, Y.D., 2002, Ammonoid succession of the Setorym River (Verkhoyansk area) and
1137 the problem of the Permian–Triassic boundary in Boreal realm: Journal of China
1138 University of Geosciences, v. 13, no. 2, p. 107–123.
1139 Zakharov, Y.D., and Popov, A.M., 2014, Recovery of brachiopod and ammonoid faunas
1140 following the end-Permian crisis: additional evidence from the Lower Triassic of the
1141 Russian Far East and Kazakhstan: Journal of Earth Science, v. 25, no. 1, p. 1–44.
1142 Zhang, K., Tong, J., Shi, G., Lai, X., Yu, J., He, W., Peng, Y., and Jin, Y, 2007, Early Triassic
1143 conodont-palynological biostratigraphy of the Meishan D Section in Changxing,
1144 Zhejiang Province, South China: Palaeogeography, Palaeoclimatology, Palaeoecology, v.

252, p. 4–23.

Zhang, Z., He, W., Zhang, Y., Yang, T., and Wu, S., 2009, Late Permian-earliest Triassic ammonoid sequences from the Rencunping section, Sangzhi County, Hunan Province, South China and their regional correlation: Geological Science and Technology Information, v. 28, p. 23–30.

Zhao, J., Liang, X., and Zheng, Z., 1978, Late Permian cephalopods from South China: Palaeontologia Sinica, Series B, 194 p.

Zhao, L., Orchard, M.J., Tong, J., Sun, Z., Zuo, J., Zhang, S., and Yun, A., 2007, Lower Triassic conodont sequence in Chaohu, Anhui Province, China and its global correlation: Palaeogeography, Palaeoclimatology, Palaeoecology, v. 252, p. 24–38.

Zheng, Z, 1981, Uppermost Permian (Changhsingian) ammonoids from Western Guizhou: Acta Palaeontologica Sinica, v. 20, p. 107–114.

Figure captions

Figure 1. (**1**) Early Triassic paleogeographic map of South China, modified from Feng et al. (1997), Lehrmann et al. (1998) and Bagherpour et al. (2017). NPJB: Nanpanjiang Basin. Note that the exact paleogeography of the southern part of the NPJB is controversial (see Bagherpour et al. 2017). (**2**) Early Triassic paleogeographic reconstruction of Tethys, Pangea and Panthalassa, modified from Scotese (2001).

Figure 2. View of the Gujiao section.

Figure 3. Distribution of ammonoid taxa in the Gujiao section. Open dots indicate occurrences based on fragmentary or poorly preserved specimen.

Figure 4. (**1–11**) *Ophiceras medium* Griesbach, 1880. (**1**) YFMCUG 00001, from GJ-15. (**2–5**) YFMCUG 00002, from GJ-15. (**6–10**) YFMCUG 00003, from GJ-15, suture line at H = 6.2 mm. (**11**) YFMCUG 00008, from GJ-28. (**12–18**) *Ophiceras* sp. indet. (**12–15**) YFMCUG 00066, from GJ-33. (**16–18**) YFMCUG 00071, from GJ-33. (**19–20**) Ophiceratidae gen. indet., YFMCUG 00010, from GJ-23, suture line at H = 13.0 mm. (**21–24**) *Vishnuites pralambha* Diener, 1897. (**21–22**) YFMCUG 00007, from GJ-25. (**23–24**) YFMCUG 00051, from GJ-33.

Figure 5. Scatter diagrams of height/diameter (H/D), width/diameter (W/D) and umbilic/diameter (U/D) for *Ophiceras medium*. Data from the Himalayas is from Diener (1897) [n=16]. White symbols indicate specimens from Gujiao section [n=4].

Figure 6. Scatter diagrams of H/D, W/D and U/D for *Ophiceras* sp. indet. [n=33].

Figure 7. (**1–16**) *Ambites radiatus* (Brühwiler et al., 2008). (**1–4**) YFMCUG 00088, from GJ-40. (**5–8**) YFMCUG 00087, from GJ-40. (**9–12**) YFMCUG 00086, from GJ-40. (**13–16**) YFMCUG 00089, from GJ-40. (**17–21**) Gyronitidae gen. indet., YFMCUG 00005, from GJ-15, suture line at H = 5.0 mm. (**22–34**) ?Gyronitidae gen. et sp. indet. (**22**) YFMCUG

00095, from GJ-40. (**23–26**) YFMCUG 00097, from GJ-40. (**27–30**) YFMCUG 00098, from GJ-40. (**31–32**) YFMCUG 00094, from GJ-40. (**33–34**) YFMCUG 00096, from GJ-40.

Figure 8. Scatter diagrams of H/D, W/D and U/D for *Ambites radiatus* (Brühwiler et al., 2008). White symbols indicate specimens from Gujiao section [n=7], and gray symbols indicate data from Ware et al. (in press) [n=55].

Figure 9. Scatter diagrams of H/D, W/D and U/D for ?Gyronitidae gen. et sp. indet. [n=7].

Figure 10. *Jieshaniceras guizhouense* (Zakharov and Mu in Mu et al., 2007). (**1–4, 16**) YFMCUG 00009, from GJ-33, suture line at H=22.3 mm. (**5–7**) YFMCUG 00013, from GJ-33. (**8–9**) YFMCUG 00010, from GJ-33. (**10–12**) YFMCUG 00014, from GJ-35. (**13–15**) YFMCUG 00012, from GJ-33, suture line at H=12.1 mm. (**17–19**) YFMCUG 00015, from GJ-35, suture line at H = 30.4 mm.

Figure 11. (**1–6**) *Jieshaniceras guizhouense* (Zakharov and Mu in Mu et al., 2007). (**1–3**) YFMCUG 00045, from GJ-35. (**4**) YFMCUG 00046, from GJ-35, suture line at H = 24.8 mm. (**5**) YFMCUG 00047, from GJ-35, suture line at H=24.3 mm. (**6**) YFMCUG 00043, from GJ-35, suture line at H=24.0 mm. (**7–11**) *Proptychites* sp. indet. (**7–9**) YFMCUG 00049, from GJ-35, Suture line at H=23.8 mm. (**10–11**) YFMCUG 00050, from GJ-40.

Figure 12. Scatter diagrams of H/D, W/D and U/D for *Jieshaniceras guizhouense* (Zakharov

and Mu in Mu et al., 2007). Data from Mu et al., 2007 [n=21], Brühwiler et al., 2008 [n=9] and this work [n=6]. White symbols indicate specimens from Gujiao section.

Figure 13. (**1–11**) *Pseudoproptychites* cf. *hiemalis*. (**1–3**) YFMCUG 00090, from GJ-40. (**4–5**) YFMCUG 00091, from GJ-40. (**6–7**) YFMCUG 00092, from GJ-40. (**8–11**) YFMCUG 00093, from GJ-40. (**12–27**) *Mullericeras gujiaoense* n. sp. (**12–14**) holotype, YFMCUG 00018, from GJ-33. (**15–17**) YFMCUG 00021, from GJ-33. (**18–21**) YFMCUG 00024, from GJ-33. (**22–24**) YFMCUG 00026, from GJ-33. (**25**) YFMCUG 00017, from GJ-33, suture line at H = 25.3 mm. (**26**) YFMCUG 00019, from GJ-33, suture line at H=24.8 mm. (**27**) YFMCUG 00016, from GJ-33, suture line at H = 24.4 mm.

Figure 14. Scatter diagrams of H/D, W/D and U/D for *Mullericeras gujiaoense* n. sp. [n=25].

Figure 15. (**1–5, 8-18**) *Ussuridiscus* cf. *varaha*. (**1–4**) YFMCUG 00100, from GJ-40. (**5**) YFMCUG 00123-2, from GJ-40. (**8**) YFMCUG 00118-3, from GJ-40. (**9**) YFMCUG 00118-2, from GJ-40. (**10–12**) YFMCUG 00101, from GJ-40. (**13–15**) YFMCUG 00102, from GJ-40. (**16**) YFMCUG 00109, from GJ-40. (**17–18**) YFMCUG 00125, from GJ-40. (**6**) *Ambites radiatus* (Brühwiler et al., 2008), YFMCUG 00123-1, from GJ-40. (**7**) ?Gyronitidae gen. et sp. indet., YFMCUG 00118-1, from GJ-40. (**19**) ?Mullericeratidae gen. indet., YFMCUG 00004, from GJ-15.

Figure 16. Scatter diagrams of H/D, W/D and U/D for *Ussuridiscus* cf. *varaha* [n=33].

Figure 17. Partly preserved suture lines of *Ussuridiscus* cf. *varaha* showing an auxiliary saddle (white arrow).

Figure 18. Induan ammonoid zonation of South China and global correlation.

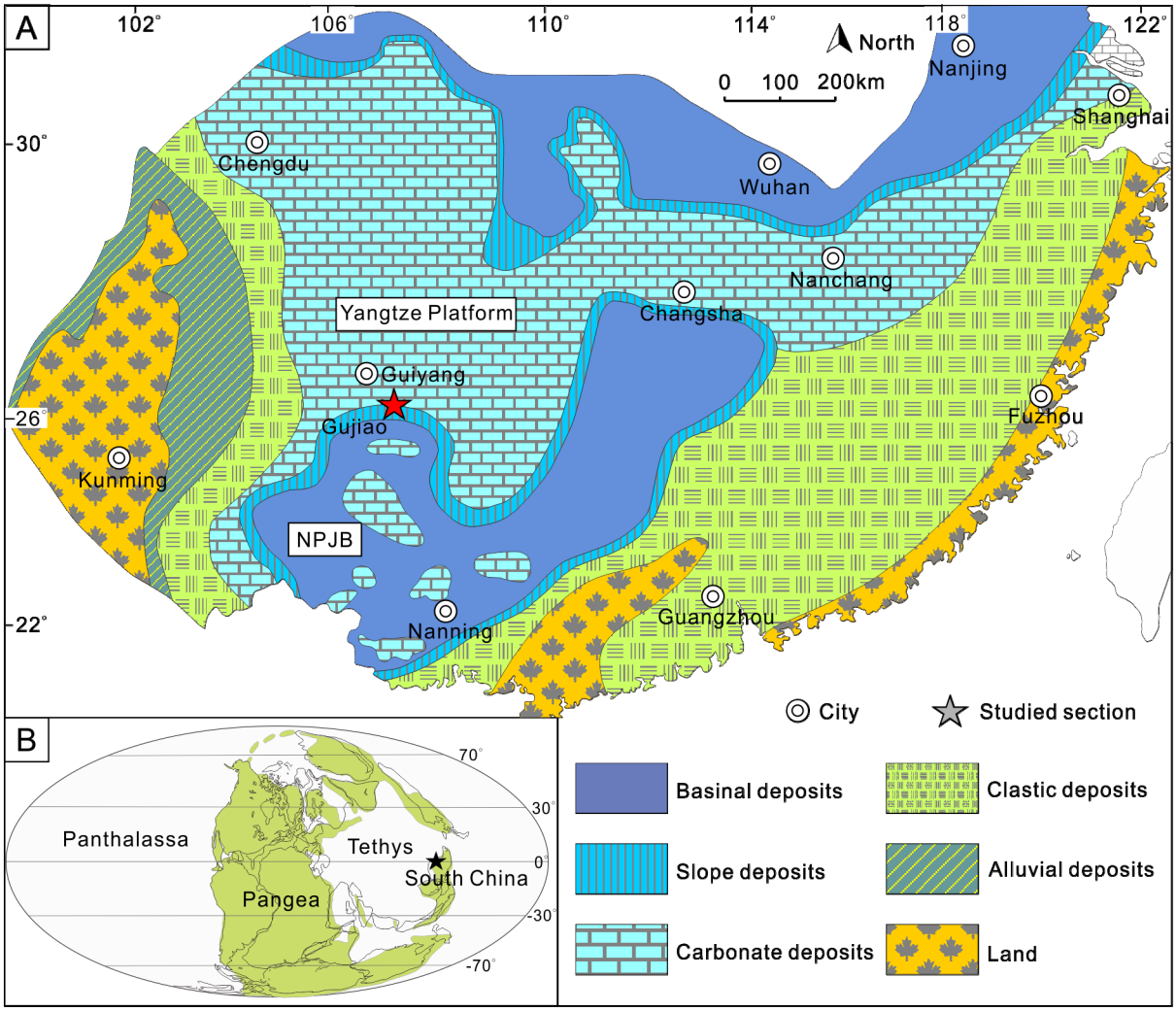

Figure 1. A, Early Triassic paleogeographic map of South China modified from Feng *et al*. (1997), Lehrmann *et al*. (1998) and Bagherpour *et al*. (2017). NPJB. Nanpanjiang Basin. **B,** Early Triassic paleogeographic reconstruction of Tethys, Pangea and Panthalassa, modified from Scotese (2001).

Figure 2. Landscape view of the Gujiao section.

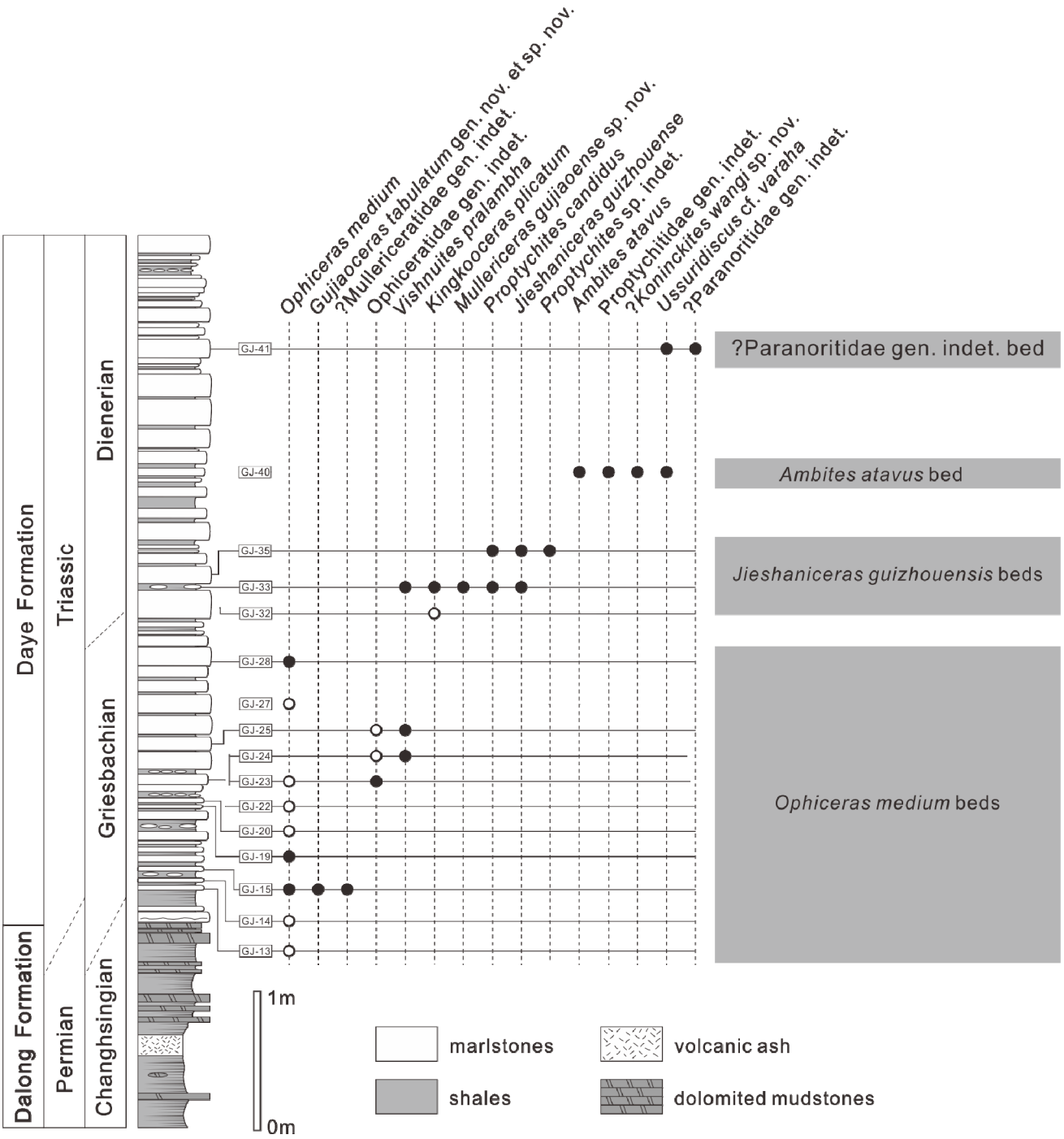

Figure 3. Distribution of ammonoid taxa in the Gujiao section. Open dots indicate occurrences based only on fragment or poorly preserved specimen.

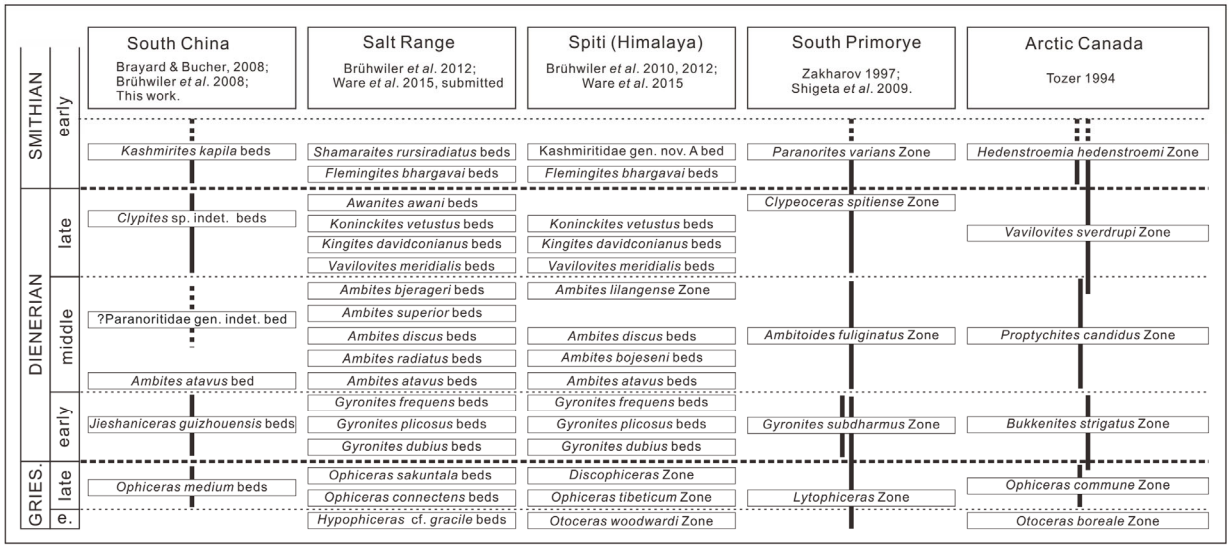

Figure 4. Induan ammonoid zonation of South China and worldwide correlation.

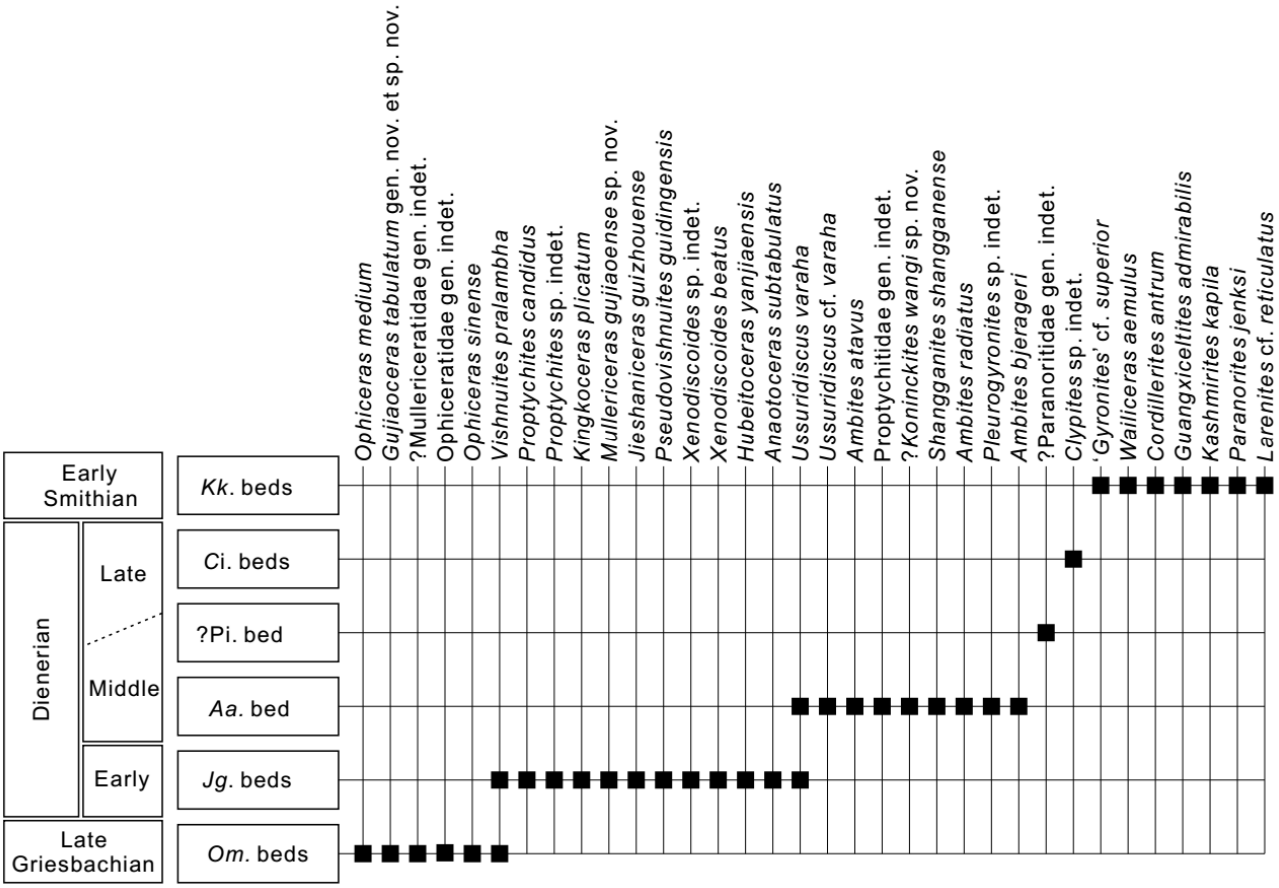

Figure 5. Synthetic range chart showing the distribution of Induan and early Smithian ammonoid taxa in South China (data from Xu 1988; Mu *et al*. 2007; Brühwiler *et al*. 2008; Brayard & Bucher 2008 and this work). *Om*.: *Ophiceras medium*; *Jg*.: *Jeishaniceras guizhouensis*; *Aa*.: *Ambites atavus*; ?Pi.: ?Paranoritidae gen. indet.; *Ci*.: *Clypites* sp. indet.; *Kk*.: *Kashmirites kapila*.

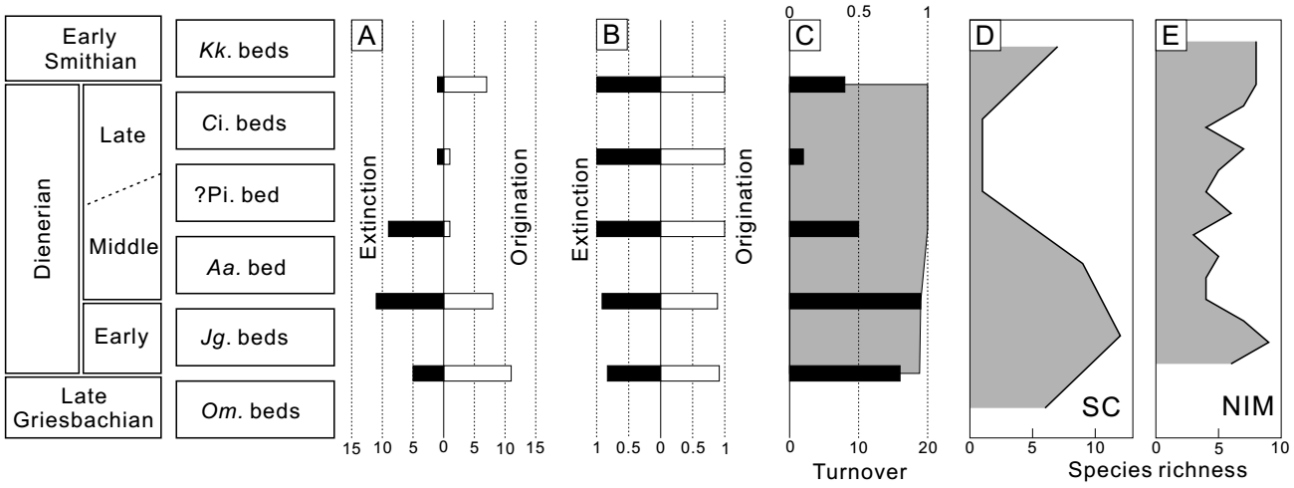

Figure 6. A, Number of ammonoid species extinction and origination; **B,** Percentages of ammonoid species extinction and origination; **C,** Number (bars) and percentages (shaded areas) of turnovers; **D,** Species richness of South China (SC) and North Indian Margin (NIM), the data of NIM from Ware *et al*. (2015). Uncertain taxonomic assignment were counted in richness analyses when taxa are clearly different from other co-occurring taxa. Species richness represents the number of species in the beds or bed. Originations and extinctions respectively correspond to the number of species that appear and disappear between two successive beds or bed. Origination rate is the number of originations divided by the species richness of the subsequent beds or bed; extinction rate is the number of extinctions divided by the species richness of the previous beds or bed. The turnover corresponds to the sum of originations and extinctions, and the turnover rate is the turnover divided by the total species richness of the two corresponding successive beds or bed.

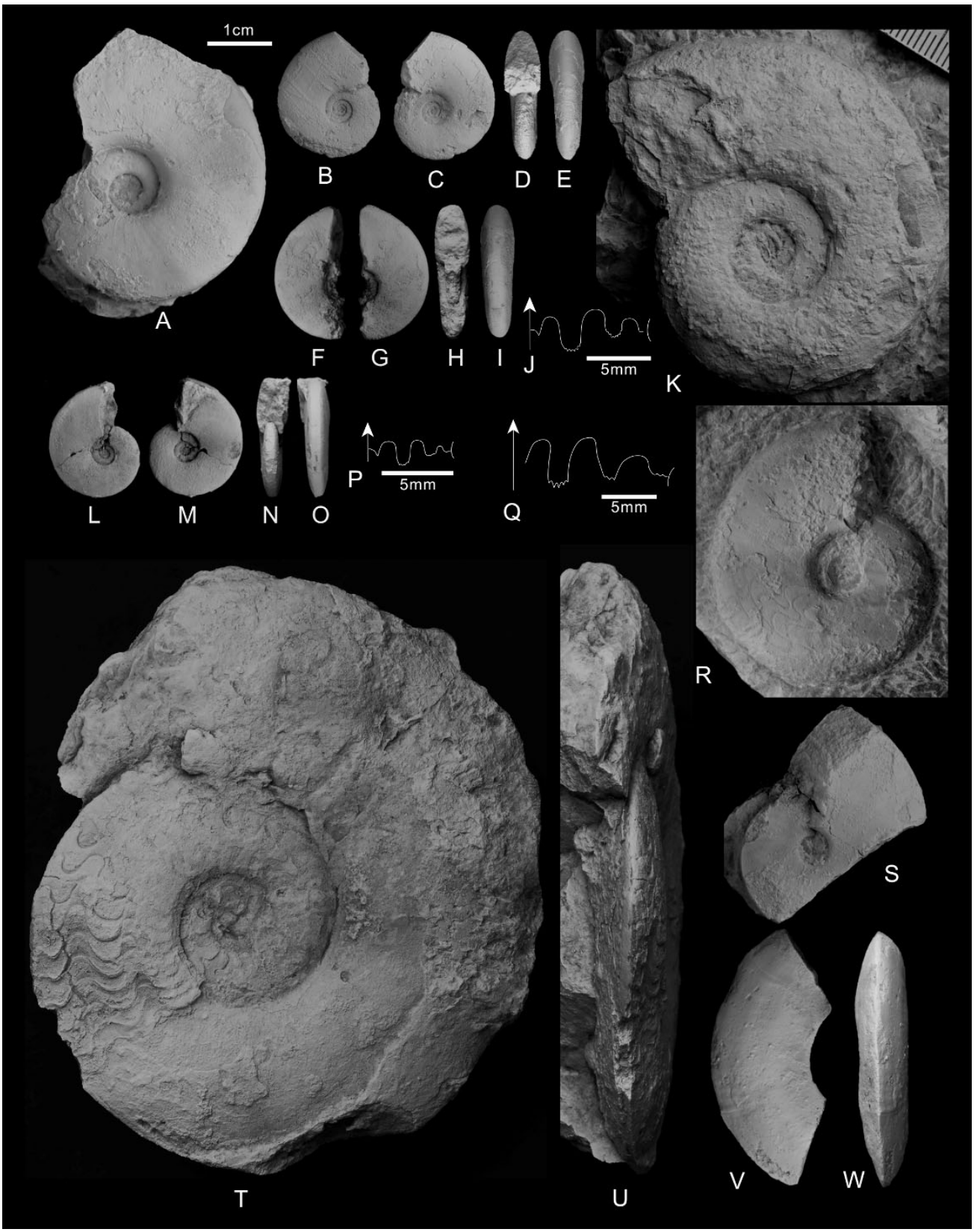

Figure 7. A-K, *Ophiceras medium* Griesbach, 1880; **A,** YFMCUG 00001, from GJ-15; **B-E,** YFMCUG 00002, from GJ-15; **F-J,** YFMCUG 00003, from GJ-15; **K,** YFMCUG 00008, from GJ-28. **L-P,** *Gujiaoceras tabulatum* gen. nov. et sp. nov., holotype, YFMCUG 00005, from GJ-15. **Q-R,** Ophiceratidae gen. indet., YFMCUG 00010, from GJ-23. **S,** ?Mullericeratidae gen. indet.,

YFMCUG 00004, from GJ-15. **T-U,** *Vishnuites pralambha* Diener, 1897; **V-W,** YFMCUG 00051, from GJ-33.

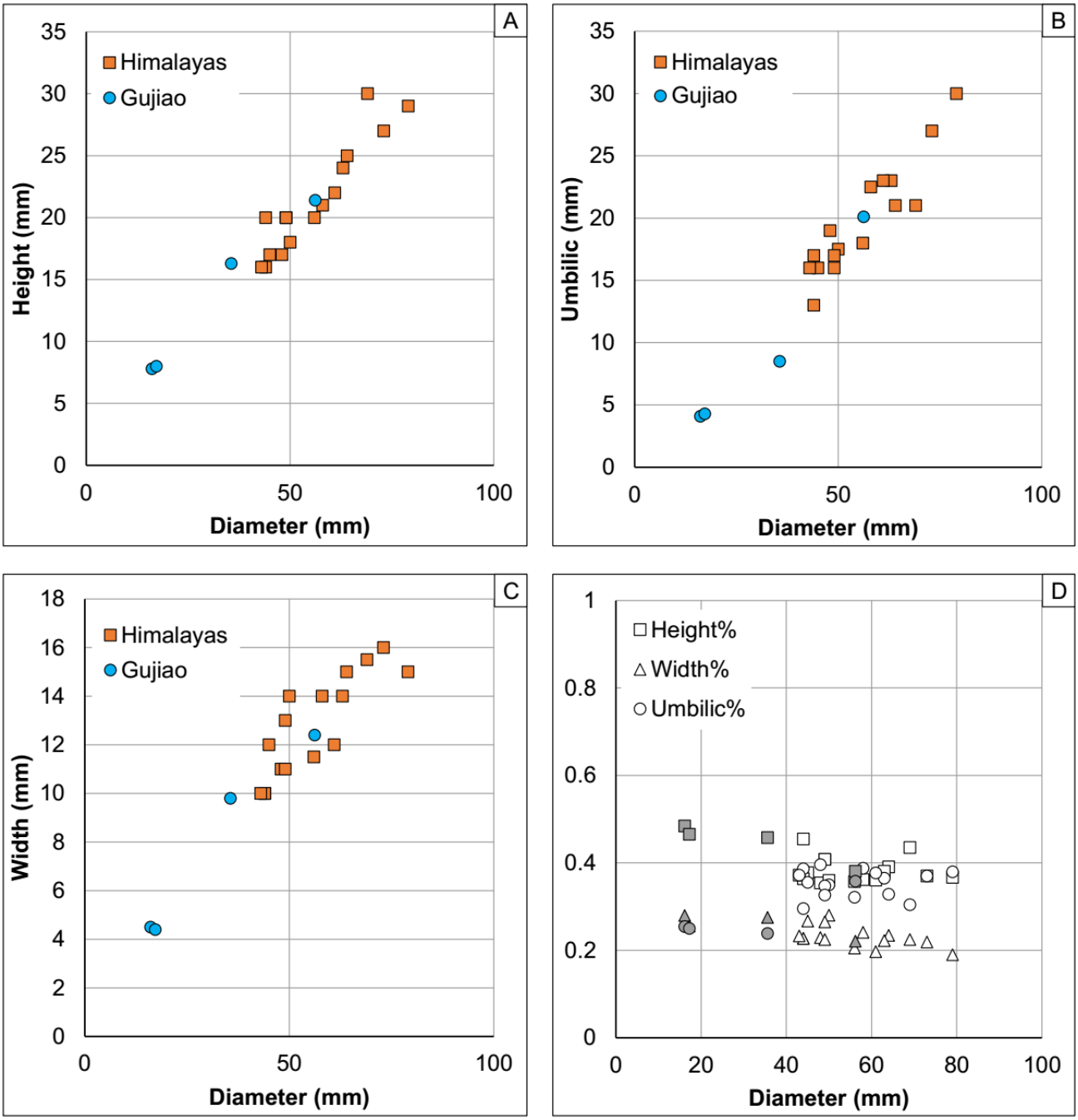

Figure 8. Scatter diagrams of height (H), width (W) and umbilic (U), and of height/diameter (H/D), width/diameter (W/D) and umbilic/diameter (U/D) for *Ophiceras medium*. Data from Himalayas is from Diener (1897). Gray symbols in diagram D indicate specimens from Gujiao section.

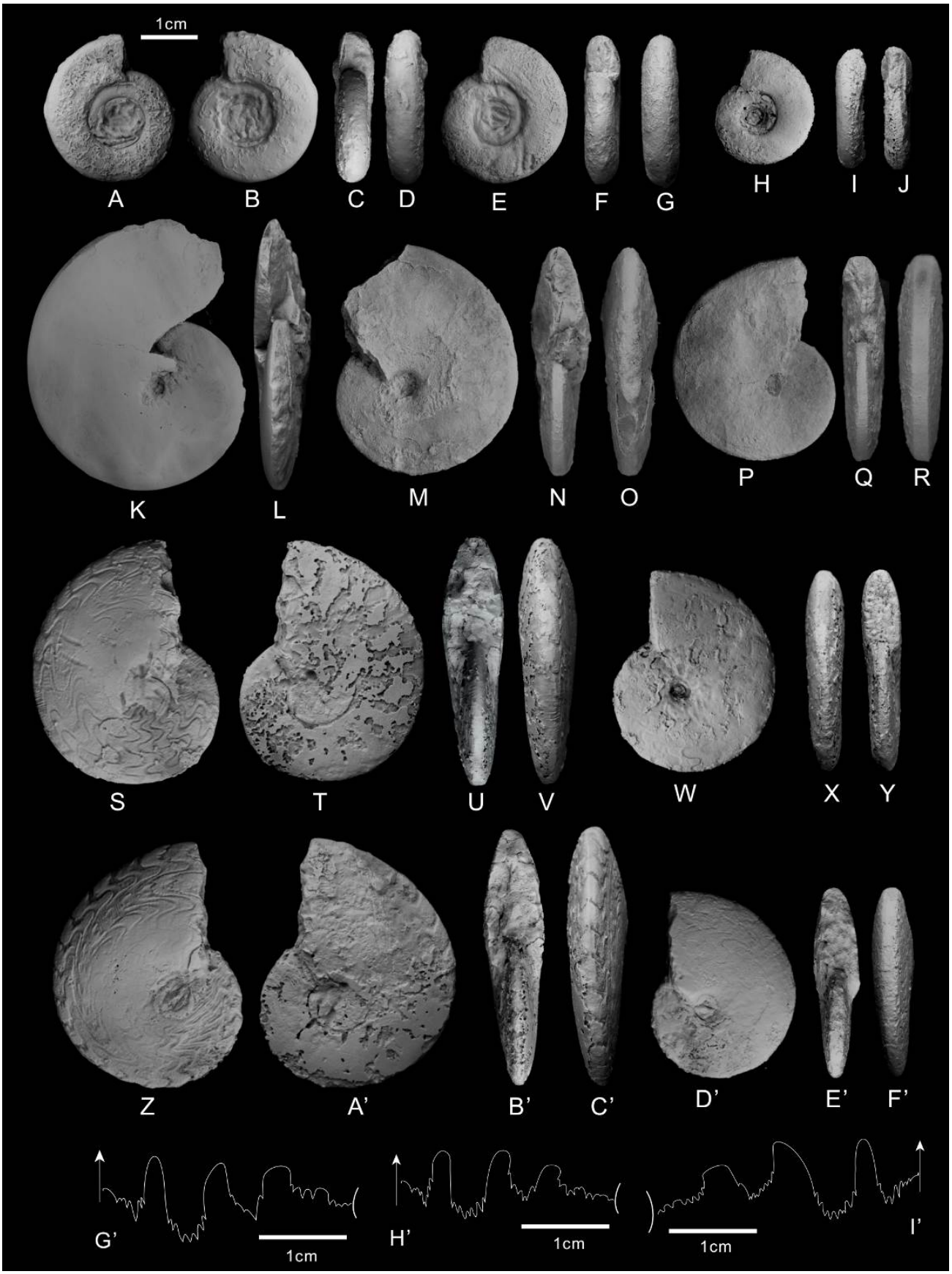

Figure 9. A-J, *Kingkooceras plicatum* gen. nov. (Xu, 1988); **A-D,** YFMCUG 00067, from GJ-33; **E-G,** YFMCUG 00066, from GJ-33; **H-J,** YFMCUG 00071, from GJ-33. **K-I',** *Mullericeras*

gujiaoense sp. nov.; **K-L, G',** YFMCUG 00017, from GJ-33; **M-O,** holotype, YFMCUG 00018, from GJ-33; **P-R,** YFMCUG 00021, from GJ-33; **S-V,** YFMCUG 00024, from GJ-33; **W-Y,** YFMCUG 00026, from GJ-33; **Z-C',** YFMCUG 00028, from GJ-33; **D'-F',** YFMCUG 00031, from GJ-33; **H',** suture line, YFMCUG 00019, from GJ-33; **I',** suture line, YFMCUG 00016, from GJ-33.

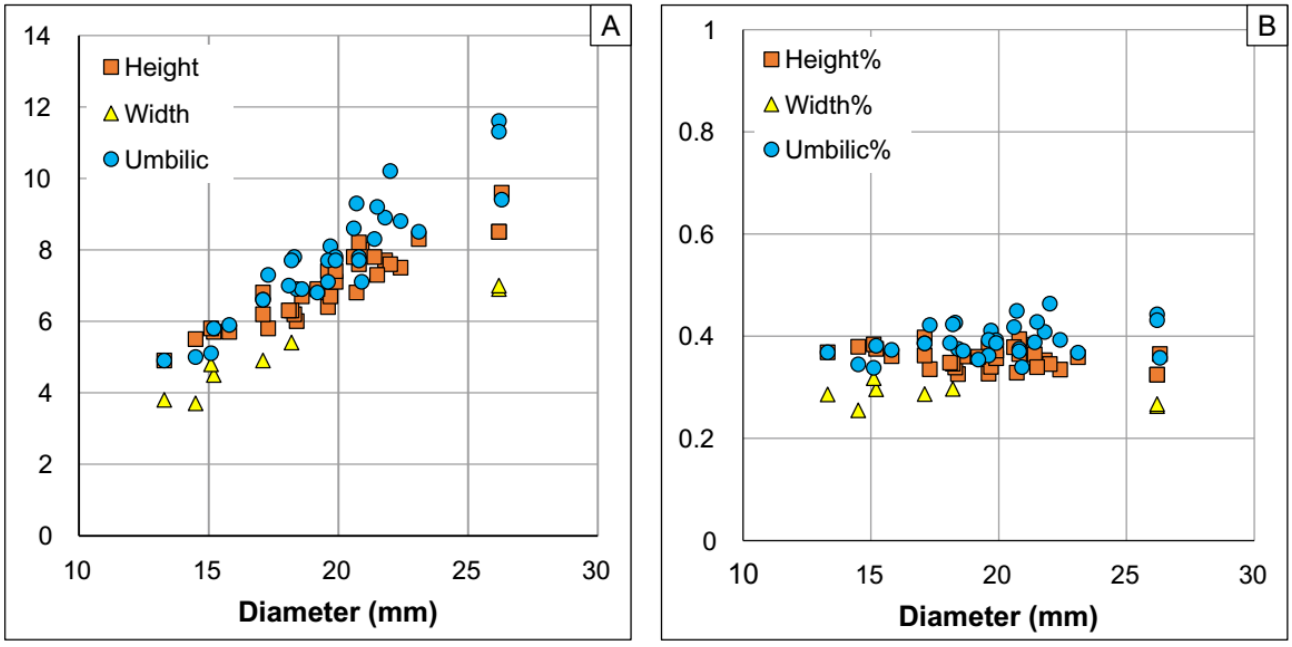

Figure 10. Scatter diagrams of H, W and U, and of H/D, W/D and U/D for *Kingkooceras plicatum* gen. nov. (Xu, 1988) [n=33].

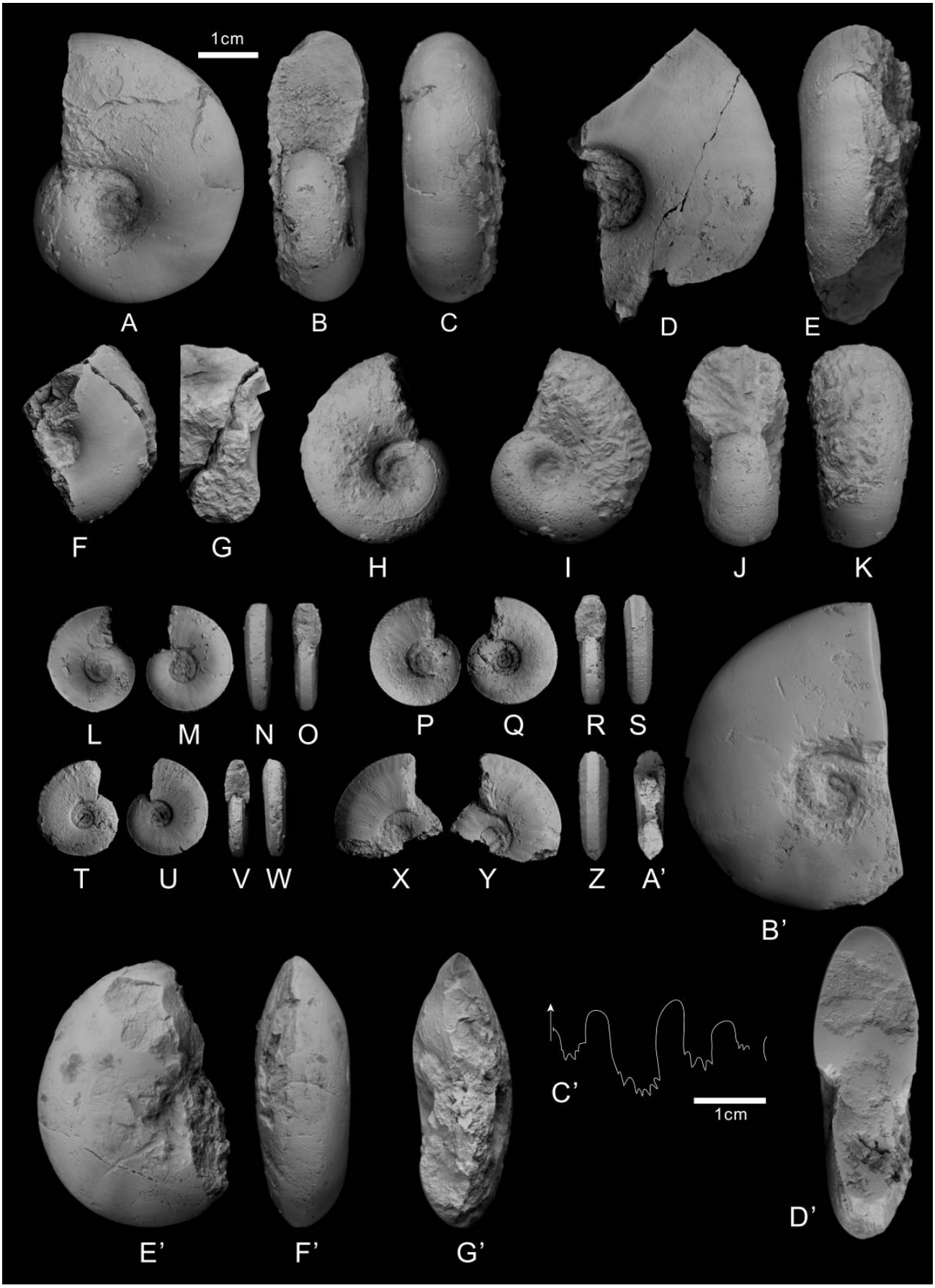

Figure 11. A-K, Proptychitidae gen. indet.; **A-C,** YFMCUG 00090, from GJ-40; **D-E,** YFMCUG

00091, from GJ-40; **F-G,** YFMCUG 00092, from GJ-40, **H-K,** YFMCUG 00093, from GJ-40. **L-A',** *Ambites atavus* (Waagen, 1895); **L-O,** YFMCUG 00088, from GJ-40; **P-S,** YFMCUG 00087, from GJ-40; **T-W,** YFMCUG 00086, from GJ-40; **B'-G',** *Proptychites* sp. indet.; **B'-D',** YFMCUG 00049, from GJ-35; **E'-F',** YFMCUG 00050, from GJ-40.

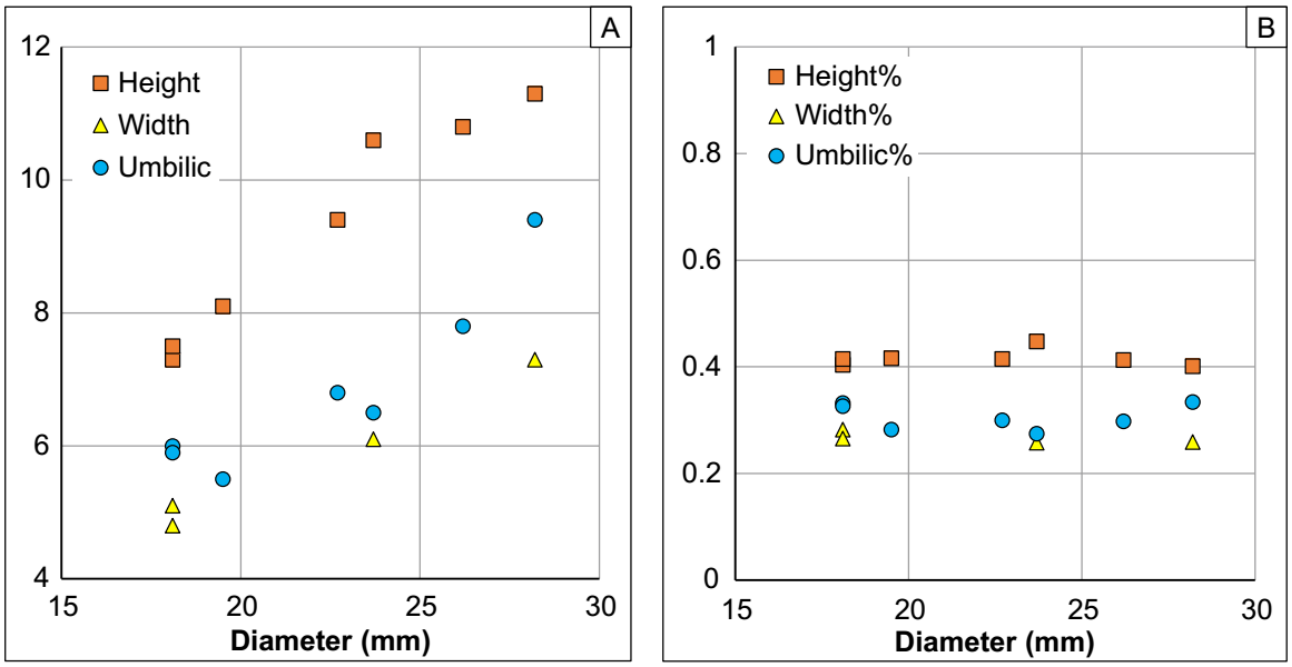

Figure 12. Scatter diagrams of H, W and U, and of H/D, W/D and U/D for *Ambites atavus* (Waagen, 1895) [n=7].

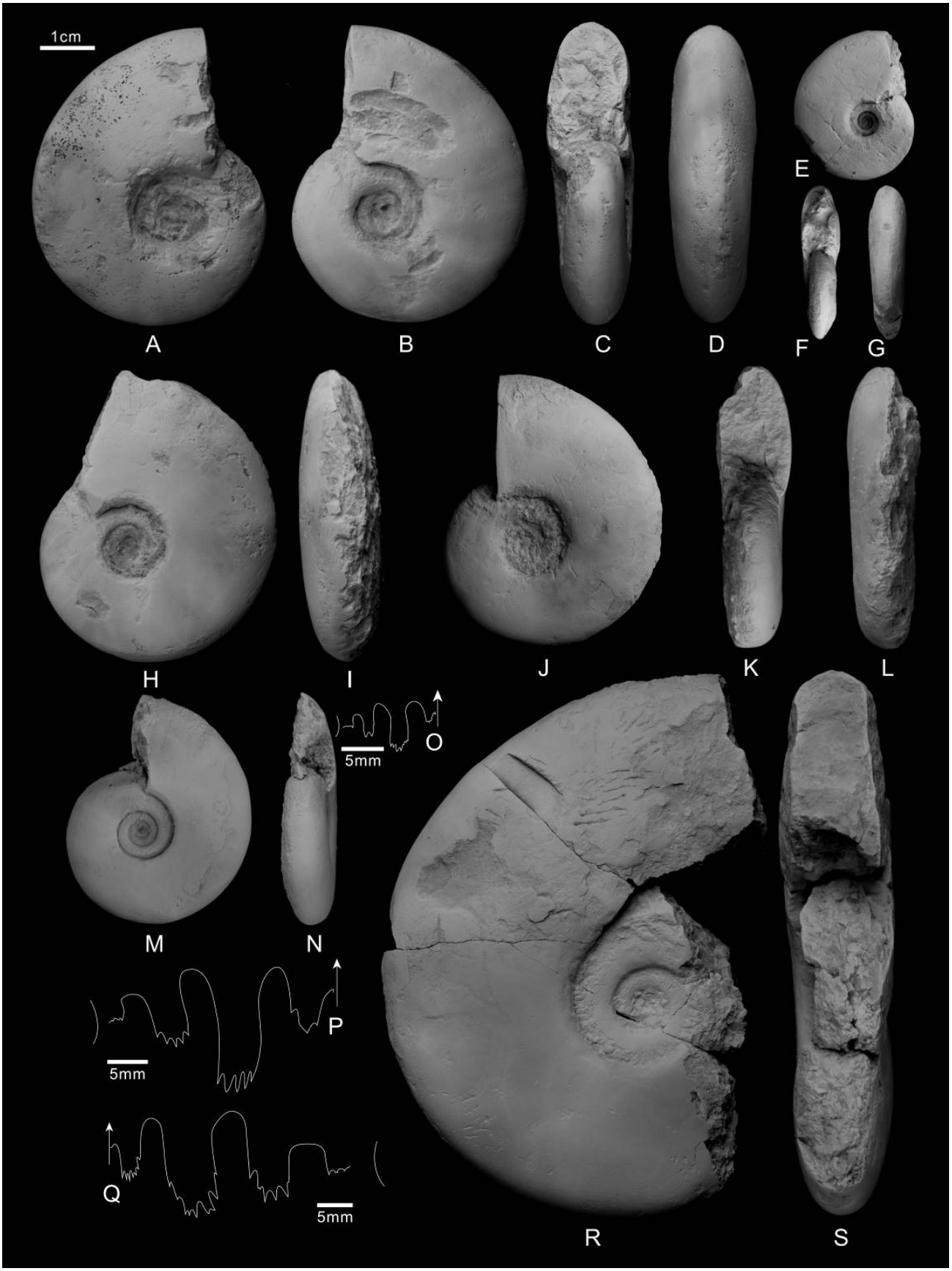

Figure 13. *Proptychites candidus* Tozer, 1961; **A-D, P,** YFMCUG 00009, from GJ-33; **E-G,** YFMCUG 00013, from GJ-33; **H-I,** YFMCUG 00010, from GJ-33; **J-L,** YFMCUG 00014, from

GJ-35; **M-O,** YFMCUG 00012, from GJ-33; **Q-S,** YFMCUG 00015, from GJ-35.

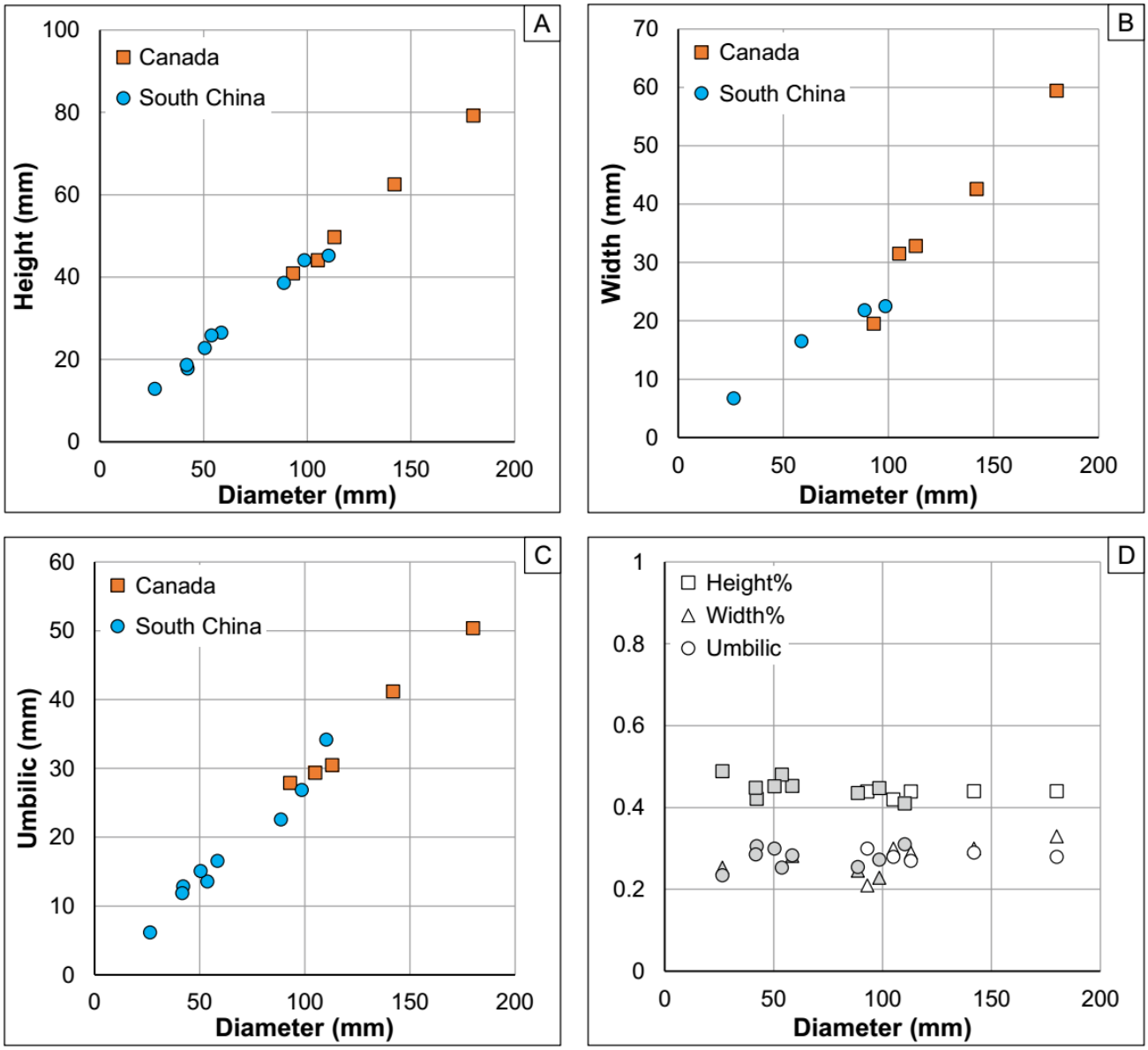

Figure 14. Scatter diagrams of H, W and U, and of H/D, W/D and U/D for *Proptychites candidus* Tozer, 1961. Data from Canada (Tozer 1994 [n=5]), South China (Brühwiler *et al*. 2008 [n=2] and this work [n=7]). The grey dots in diagram D indicate data from South China.

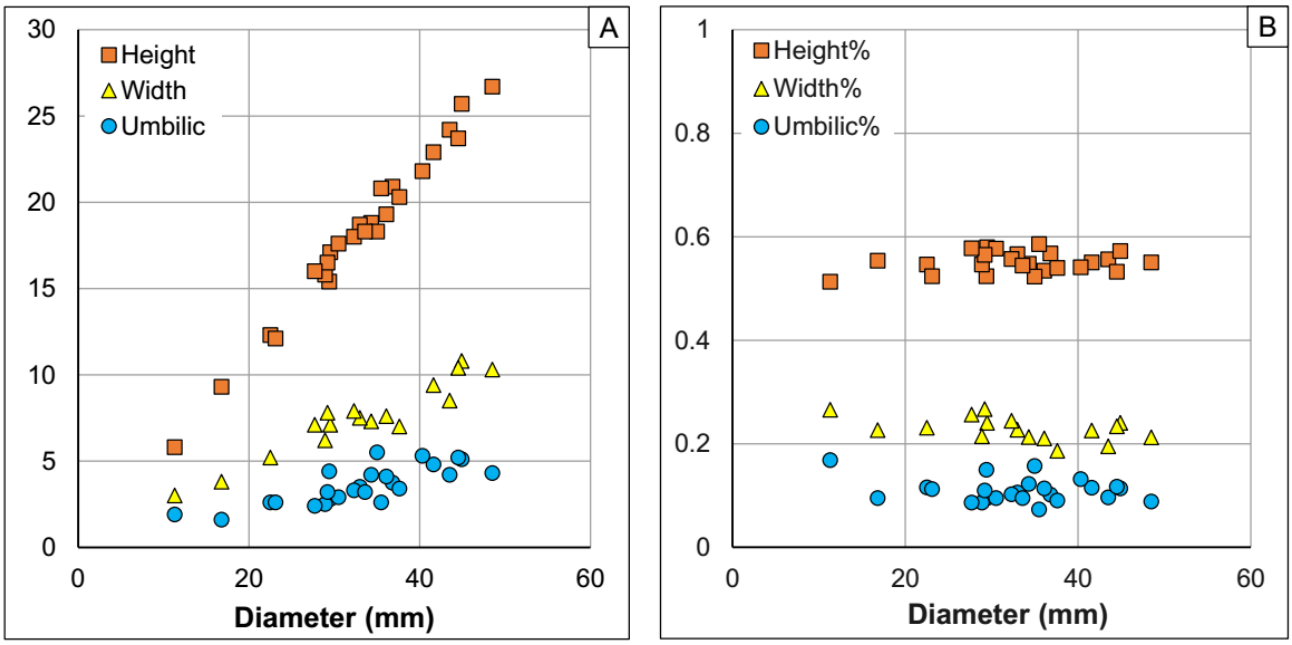

Figure 15. Scatter diagrams of H, W and U, and of H/D, W/D and U/D for *Mullericeras gujiaoense* sp. nov. [n=25].

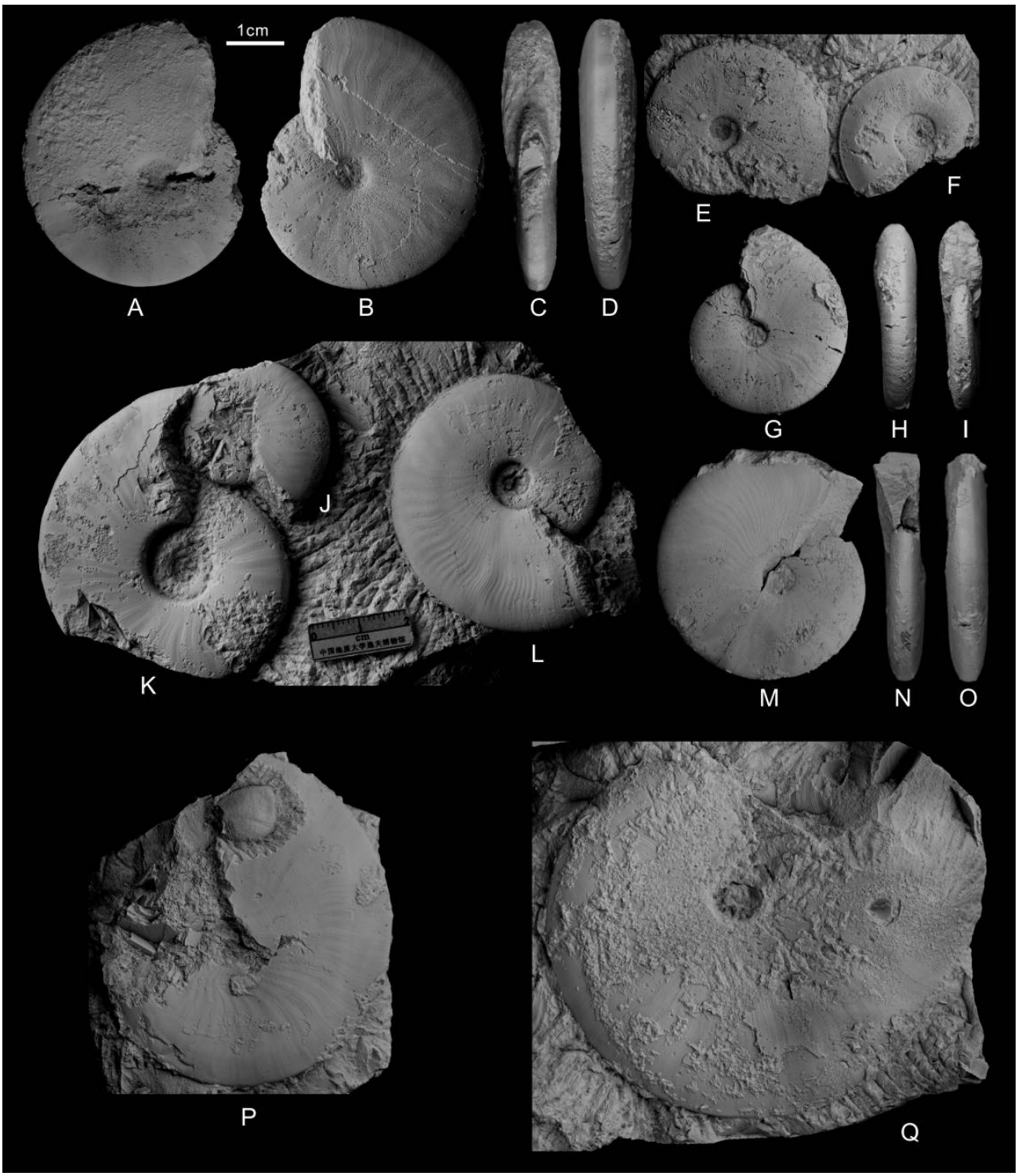

Figure 16. A-E, G-I, J, L-O, *Ussuridiscus* cf. *varaha*; **A-D,** YFMCUG 00100, from GJ-40; **E,** YFMCUG 00123-2, from GJ-40; **G-I,** YFMCUG 00101, from GJ-40; **J,** YFMCUG 00118-3, from GJ-40; **L,** YFMCUG 00118-2, from GJ-40; **M-O,** YFMCUG 00102, from GJ-40. **F,** *Ambites atavus* (Waagen, 1895), YFMCUG 00123-1, from GJ-40. **K,** ?*Koninckites wangi* sp. nov., YFMCUG 00118-1, from GJ-40. **P-Q,** ?Paranoritidae gen. indet.; **P,** YFMCUG 00128, from GJ-40; **Q,** YFMCUG 00129, from GJ-40.

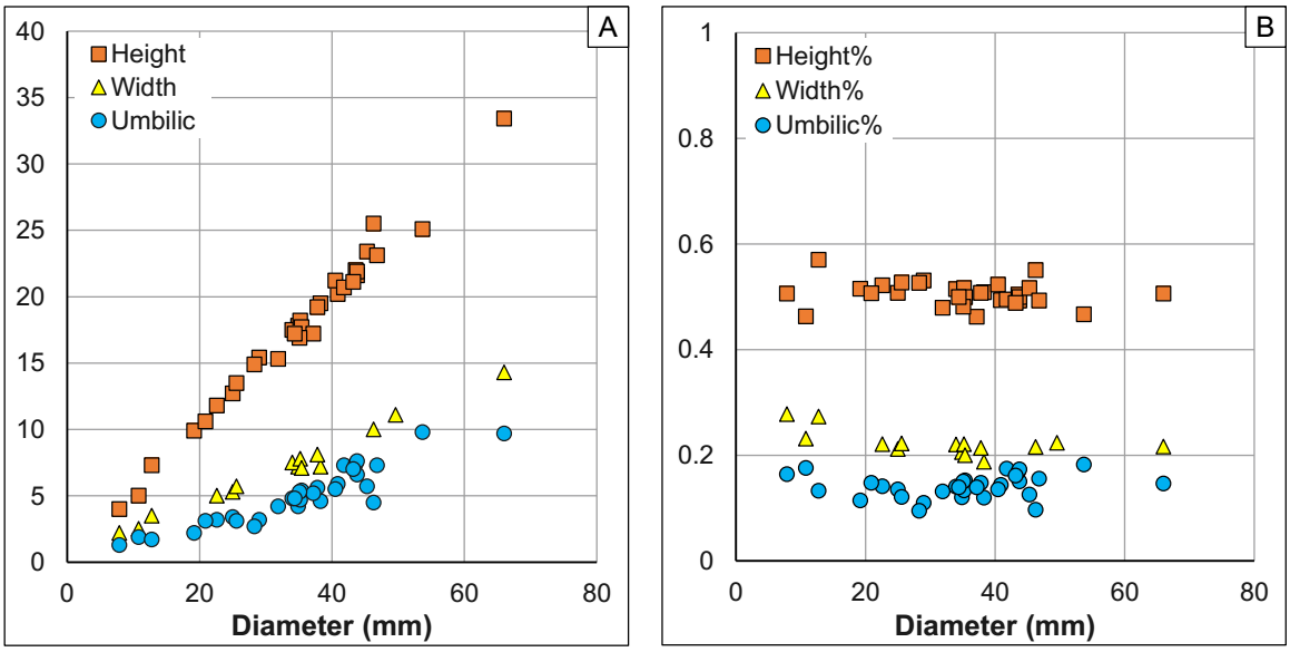

Figure 17. Scatter diagrams of H, W and U, and of H/D, W/D and U/D for *Ussuridiscus* cf. *varaha* [n=33].

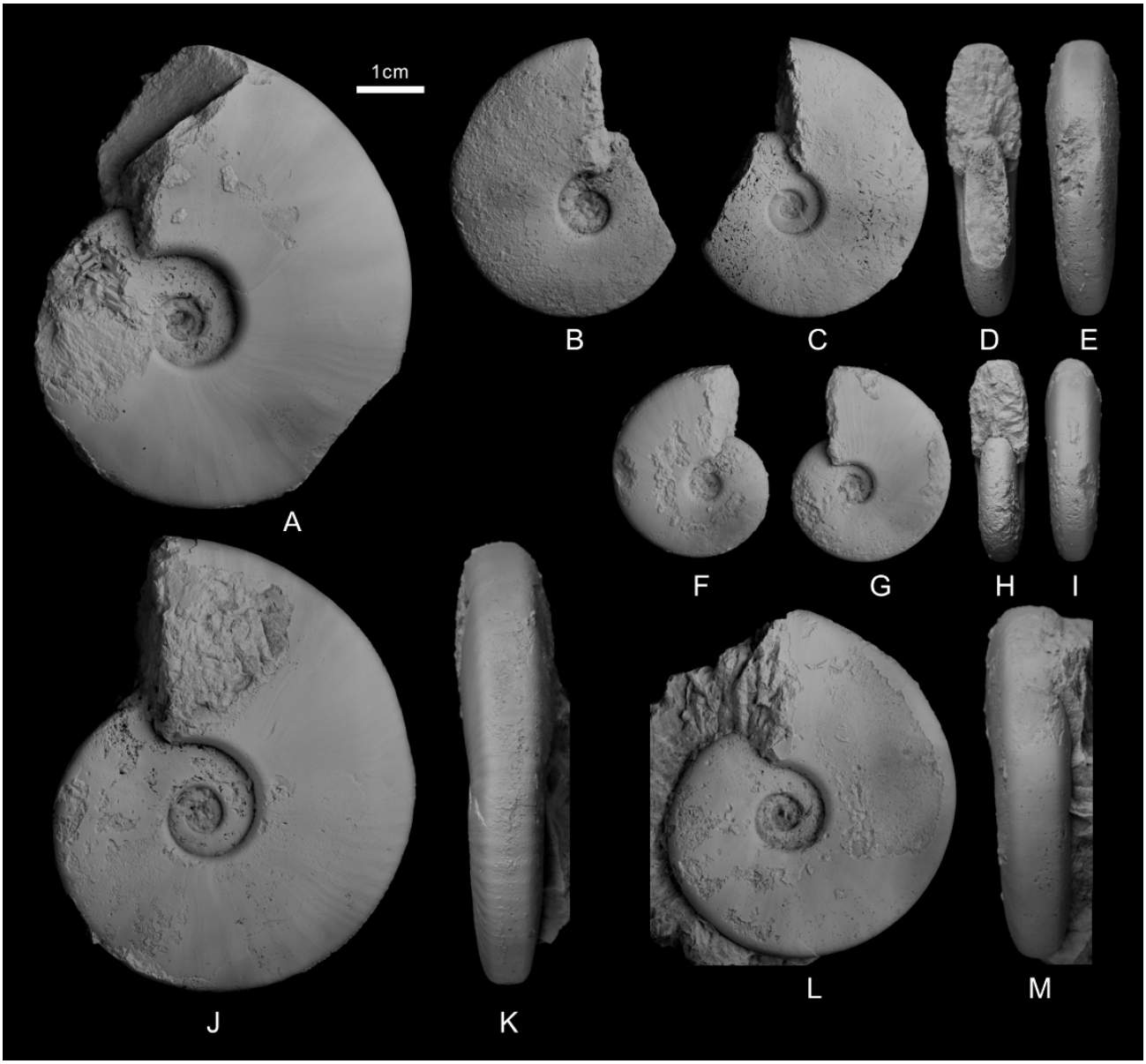

Figure 18. ?*Koninckites wangi* sp. nov.; **A,** YFMCUG 00095, from GJ-40; **B-E,** holotype, YFMCUG 00097, from GJ-40; **F-I,** YFMCUG 00098, from GJ-40; **J-K,** YFMCUG 00094, from GJ-40; **L-M,** paratype, YFMCUG 00096, from GJ-40.

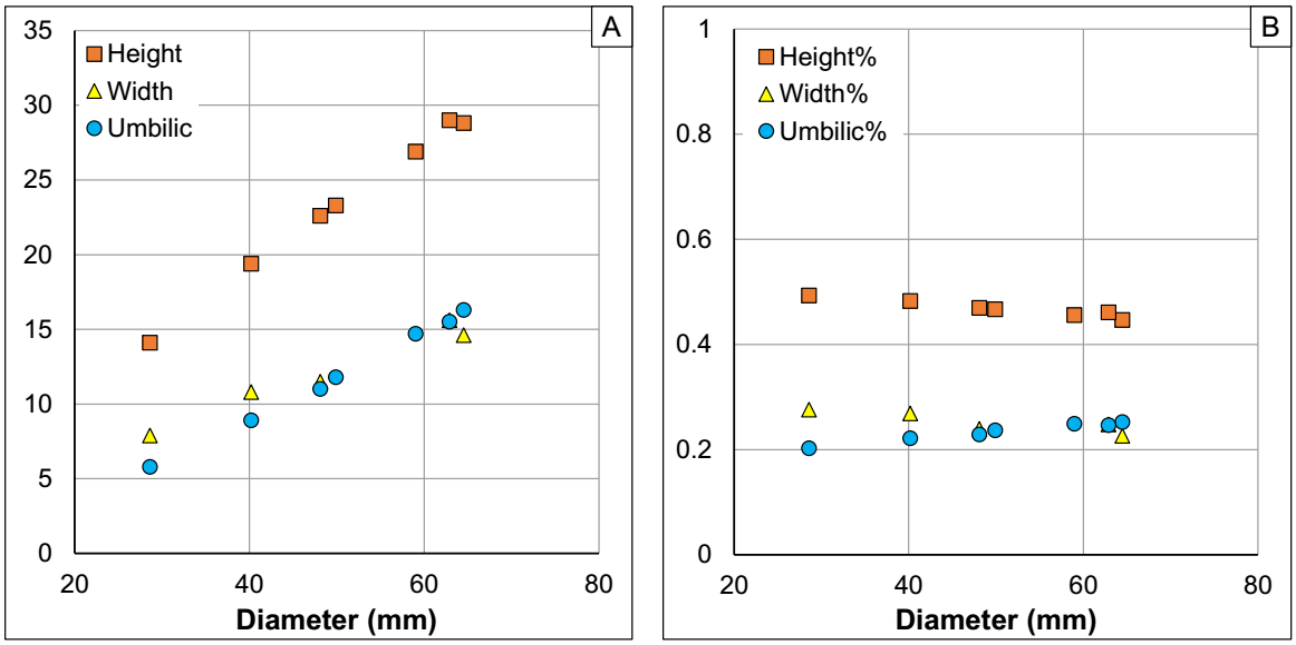

Figure 19. Scatter diagrams of H, W and U, and of H/D, W/D and U/D for ?*Koninckites wangi* sp. nov [n=7].

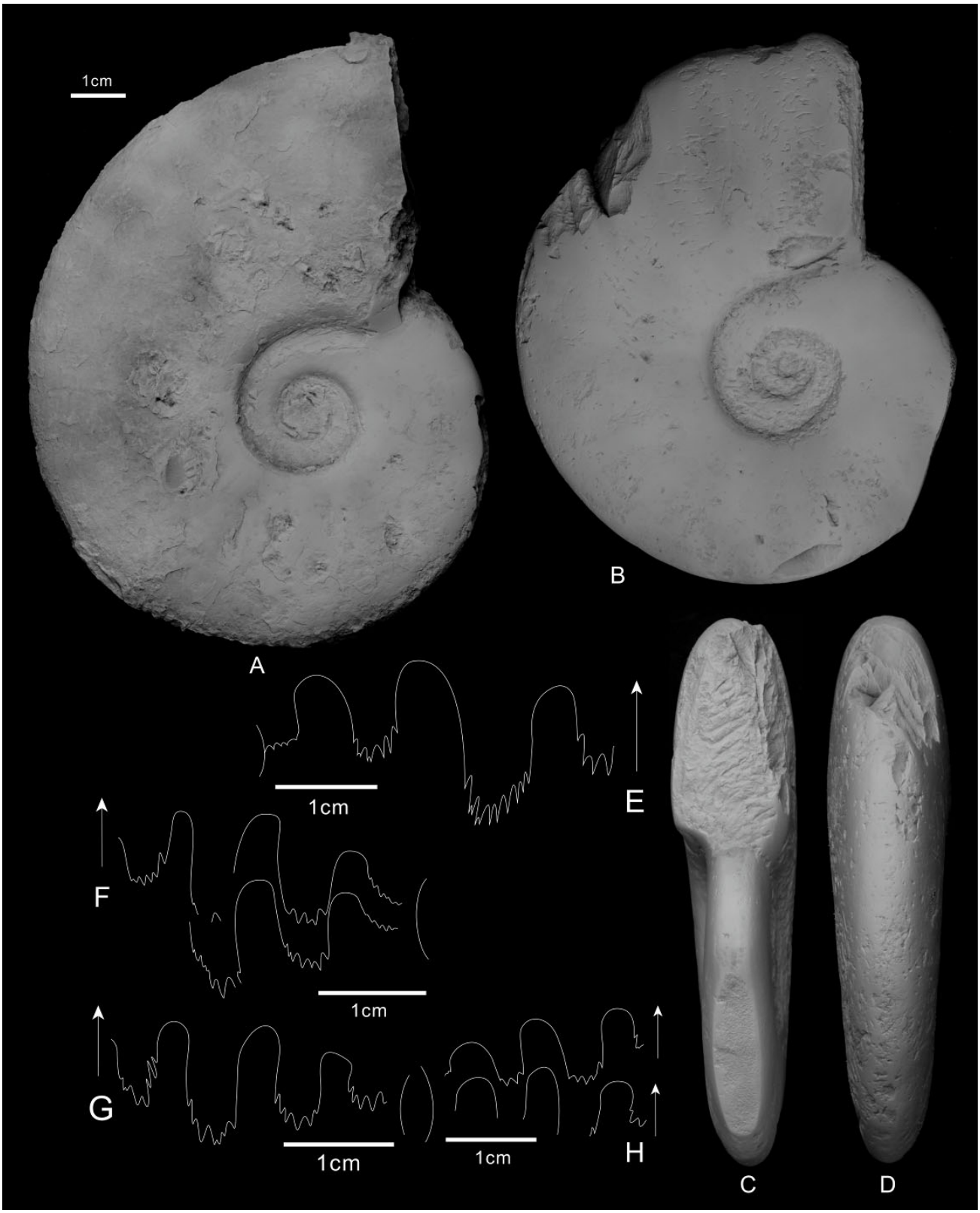

Figure 20. *Jieshaniceras guizhouense* (Zakharov & Mu *in* Mu *et al*. 2007); **A, G,** YFMCUG 00047, from GJ-35; **B-D,** YFMCUG 00045, from GJ-35; **E,** suture line, YFMCUG 00044, from GJ-35; **F,** suture line, YFMCUG 00046, from GJ-35; **H,** suture line, YFMCUG 00043, from GJ-35.

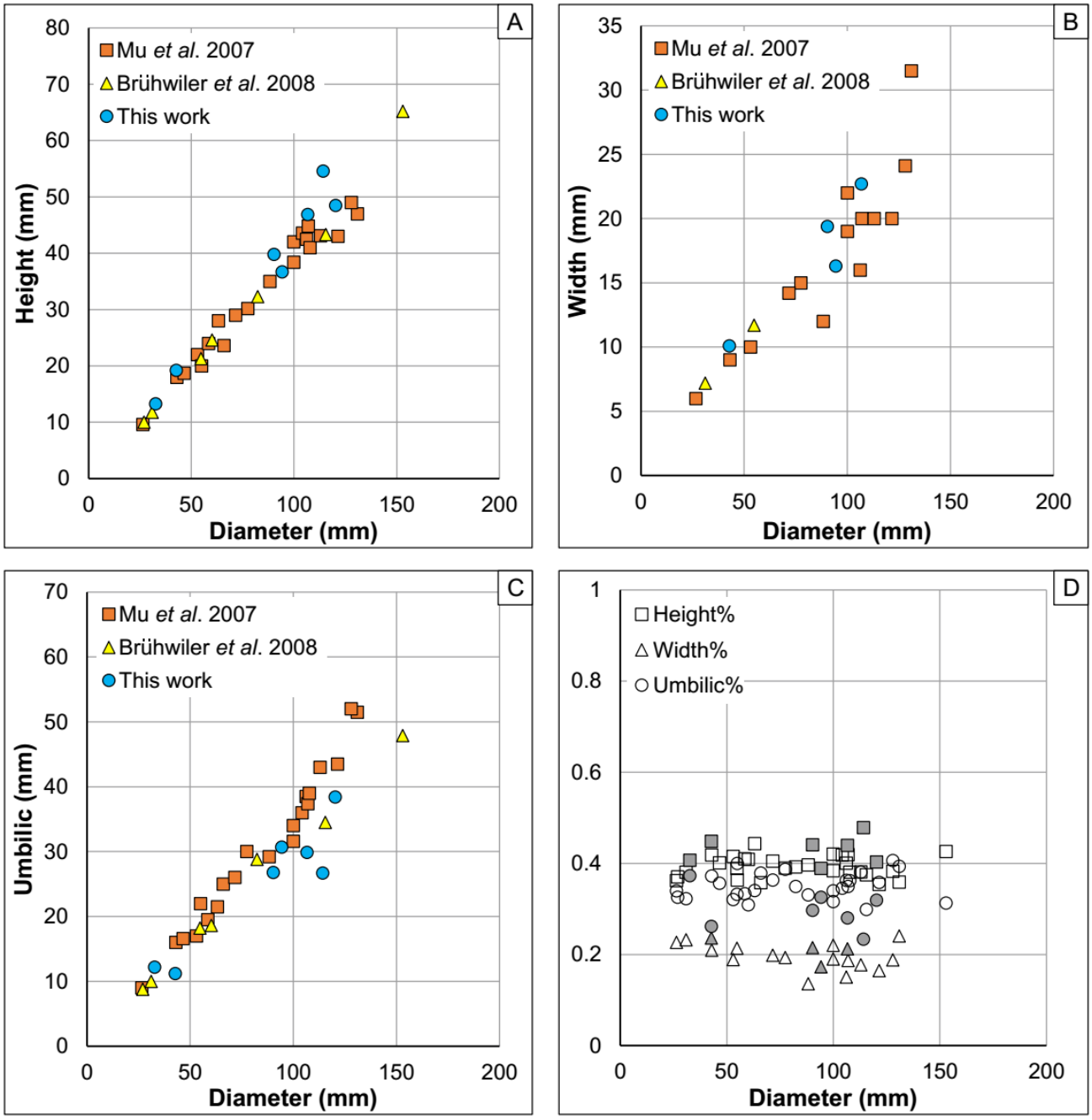

Figure 21. Scatter diagrams of H, W and U, and of H/D, W/D and U/D for *Jieshaniceras guizhouense* (Zakharov & Mu *in* Mu *et al*. 2007). Data from Mu *et al*. 2007 [n=21], Brühwiler *et al*. 2008 [n=7] and this work [n=7]. Grey symbols in the last diagram indicate specimens from Gujiao section.